Graphical Abstract

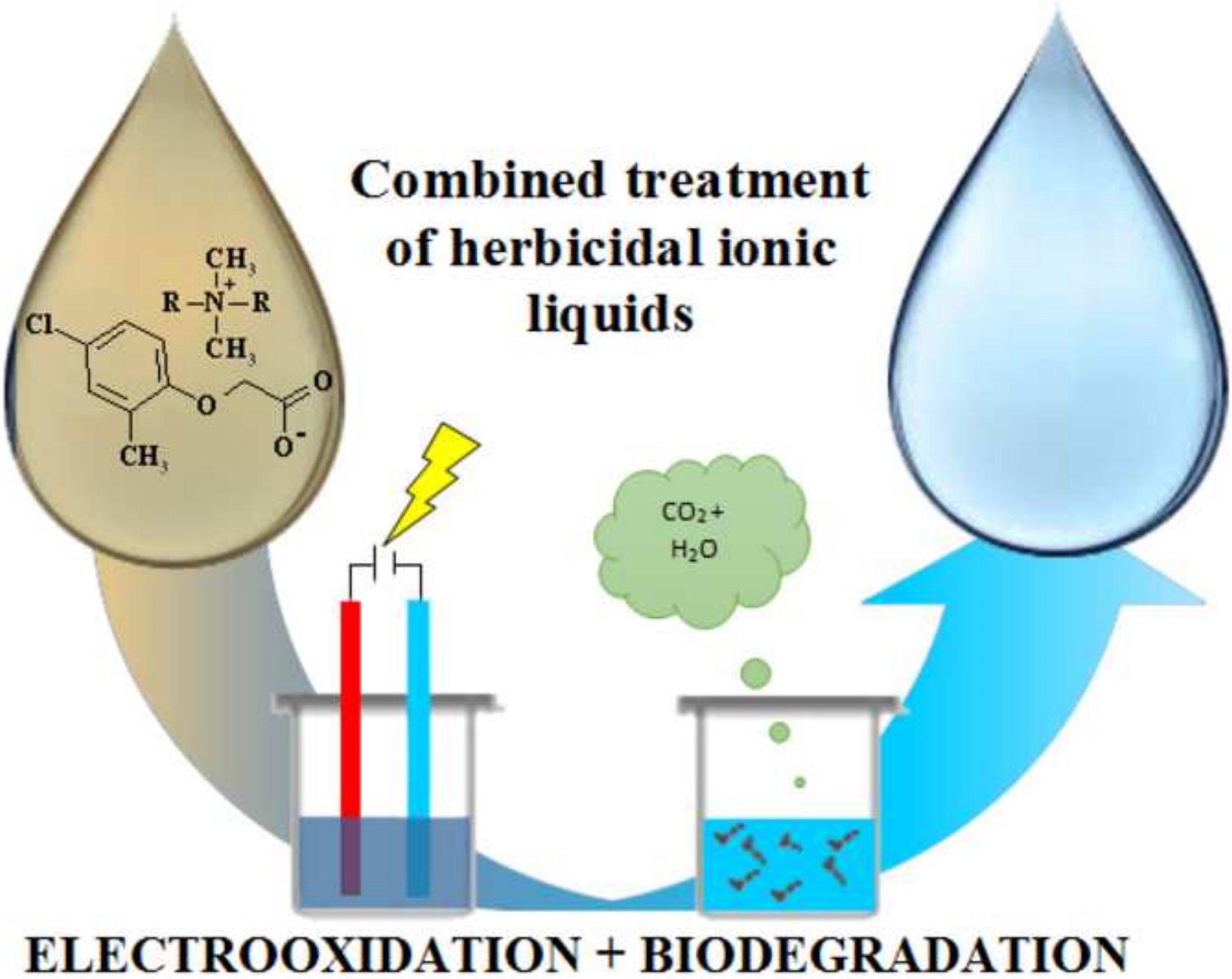

Highlights (for review)

- Novel MCPA-based herbicidal ionic liquids (HILs) were synthesized.
- Electrochemical oxidation combined with biodegradation of HILs was studied
- Oxidation efficiency of HILs ranged from 17 to 60% depending on alkyl chain length.
- Biodegradation efficiency of electrochemically-treated HILs ranged from 28 to 57.
- Biodegradation efficiency of untreated HILs ranged from 0 to 8%.

Hybrid electrochemical and biological treatment of herbicidal ionic liquids comprising the MCPA anion

Daria Pęziak-Kowalska[1], Anna Syguda[2], Łukasz Ławniczak[2], Andrzej Borkowski[3], Florence Fourcade[4], Hermann J. Heipieper[5], Grzegorz Lota[1], Łukasz Chrzanowski[2,*]

[1]Institute of Chemistry and Technical Electrochemistry, Poznan University of Technology, ul. Bedrychowo 4, 60-965 Poznan, Poland.

[2]Institute of Chemical Technology and Enginering, Poznan University of Technology, ul. Bedrychowo 4, 60-965 Poznan, Poland.

[3]Faculty of Geology, University of Warsaw, Żwirki i Wigury 93, 02-089 Warsaw, Poland.

[4]Université Rennes 1/Ecole Nationale Supérieure de Chimie de Rennes, CNRS, UMR 6226, 11 allées de Beaulieu, CS 50837, 35708 Rennes Cedex 7, France.

[5]Helmholtz Centre for Environmental Research – UFZ, Department of Environmental Biotechnology, Permoserstraße 15, D-04318 Leipzig, Germany.

[*]*Corresponding author: lukasz.chrzanowski@put.poznan.pl*

ABSTRACT

The presented study was focused on the application of an electrochemical oxidation process combined with biodegradation for the removal of novel Herbicidal Ionic Liquids (HILs) – promising protection plant products which incorporate herbicidal anions and ammonium cations. The influence of carbon chain length (n = 8, 10, 12, 14, 16, 18) in the dialkyldimethylammonium cations on electrochemical oxidation kinetics, degradation efficiency and biodegradation by activated sludge was investigated. It was established that the applied cation influenced the heterogeneous rate constant and diffusion coefficient of electrochemical oxidation. The oxidation efficiency ranged from 17% in case of HILs with C8 alkyl chain to approx. 60% in case of HILs comprising C14 and C16 alkyl chains after 3 hours of electrochemical treatment. Subsequent biodegradation studies revealed that electrochemical oxidation improved the mineralization efficiency of the studied HILs. The mineralization efficiency of electrochemically-treated HILs ranged from 28% in case of HILs comprising the C8 alkyl chain to 57% in case of HILs with C14 and C16 alkyl chains after 28 days. In case of untreated HILs, the corresponding mineralization efficiency ranged from 0 to

8%, respectively. This confirms the feasibility of a hybrid electrochemical-biological approach for treatment of herbicidal ionic liquids based on MCPA.

Keywords: electrochemical oxidation; herbicides; ionic liquids; MCPA; mineralization.

1. Introduction

Ionic liquids have gained world-wide recognition as a group of chemicals with diverse applications. Apart from typically industrial practice, ionic liquids have found use as an invaluable tool for the agricultural sector (Zajac et al., 2018). Transformation of commercial herbicides into the form of ionic liquids limits the risk of unintended transport due to volatilization. This process has recently evolved from laboratory tests to mass production, as can be seen on the example of dicamba. Monsanto introduced their line of XtendiMax products (dicamba diglycolamines) which exhibit 90% reduced volatility. Another chemical company, BASF, introduced Engenia (N,N-bis-(3-aminopropyl)methylamine salt of dicamba) with the same aim (Bomgardner, 2017). The use of herbicides in the form of herbicidal ionic liquids (HILs) has thus become reality. Nevertheless, the ionisation of herbicides does not eliminate other environmental hazards. The cations used in HILs often exhibit surface active properties which may result in increased bioavailability and toxicity to some organisms (Ławniczak et al., 2015; Piotrowska et al., 2018). HILs are also more mobile in soil and may be transferred with agricultural run-off. As a result, the study of their behaviour in the environment and development of effective treatment methods has become a necessity.

Among the possible treatment options, Advanced Oxidation Processes (AOPs) are considered as rapid and effective methods. AOPs have been successfully employed for the removal of imidazolium and pyridinium ionic liquids from aqueous systems based on e.g. ozonation (Pernak and Branicka, 2004), Ti/UV, H_2O_2/UV [6], H_2O_2/CH_3COOH/sonication process (Li et al., 2007), Fenton, Fenton-like oxidation (Siedlecka et al., 2009; Siedlecka and Stepnowski, 2009; Munoz et.al., 2015). electro-Fenton process and anodic oxidation with applied IrO_2, PbO_2, Ir/Pt, BDD electrodes (Stolte et al., 2008; Pieczyńska et al., 2015; Garcia-Segura et al., 2016). However, from a long-term perspective, this solution corresponds to considerable process costs due to energy demand.

On the other hand, biological treatment methods adhere perfectly to the policy of sustainable development. Biodegradation of organic contaminants is considered as an economically efficient and environmentally friendly alternative to chemical and physical treatment methods. Nevertheless, the mass introduction of herbicides into the environment

often renders the biodegradation processes inadequate for their complete removal. The efficiency of biodegradation processes may also be limited by the toxicity of herbicides and the fact that their chemical structures are usually not readily biodegradable.

In order to overcome the limitations of biodegradation, recent approaches suggest the use of hybrid processes. This type of treatment is based on the use of a primary physicochemical treatment process followed by secondary biological decomposition. Such combination results in a notably shorter treatment time, enhanced biodegradation efficiency and reduced process costs (Oller et al., 2011).

Electrochemical Advanced Oxidation Processes (EAOPs) can be used as pre-treatment prior to a biological process. Among them, electrooxidation and electro-Fenton are successfully studied to improve the biodegradability of aqueous effluents (Annabi et al., 2016; Ferrag-Siagh et al., 2014; Mansour et al., 2012; Yahiaoui et al., 2018). For such processes, the efficiency depends on the electrode materials. The commonly studied anodic materials in electrooxidation include active and non-active materials, with boron doped diamond (BDD) as the most popular material (Sirés et al., 2014). In case of electro-Fenton processes, carbon materials are preferred owing to their high over-potential for H_2 evolution and their low catalytic activity for hydrogen peroxide decomposition (Brillas et al., 2009). They can be also used as anode material but the applied potentials or applied current density cannot be as high as in electrooxidation. Nevertheless, the electrochemical oxidation on carbon materials can be effective for improvement of biodegradability when the pollutant is electroactive (Fontmorin et al., 2012). This was confirmed by a study focused on the removal of (2,4-dichlorophenoxy)acetic acid (2,4-D) which showed very promising results when electrochemical oxidation was coupled with biodegradation (Fontmorin et al., 2013). Similar attempts were also carried out in case of ionic liquids. For example, a first approach to combine biological degradation after the electrochemical treatment of ILs was also conducted (Stolte et al., 2008). It was noticed that the structure of the ILs influenced the efficiency of Fenton and anodic oxidation processes (Siedlecka and Stepnowski, 2009; Pieczyńska et al., 2015). Aside from the chain length of the substituent in the cation, it was established that the structure of the anion also seems to influence on the efficiency of AOP processes. This is of importance in case of herbicidal ionic liquids, in which the herbicide is usually incorporated as the anion.

We hypothesize that due to the ionic nature of HILs they may be more susceptible to electrochemical degradation, which will ultimately increase their final biodegradation efficiency. The aim of this study was to determine the efficiency of a hybrid process which

combined electrochemical oxidation and biodegradation for the treatment of HILs based on the (4-chloro-2-methylphenoxy)acetate (MCPA) anion and dialkyldimethyammonium cation.

2. Materials and methods

Materials and chemicals

The materials and reagents were purchased from Sigma-Aldrich: dimethyloctylamine (95%), decyldimethylamine (98%), dodecyldimethylamine (98%), dimethyltetradecylamine (95%), heksadecyldimethylamine (95%), 1-bromohexane (98%), 1-bromooctane (99%), 1-bromodecane (98%), 1-bromododecane (97%), 1-bromotetradecane 1-bromooctadodecane (97%), sodium tetraphenylborate (99.5%), activated carbon, (97%), from TCI: dimethyloctadecylamine (85%), from Alfa Aesar: 1-bromohexadecane (98%), from Organika Sarzyna: (4-chloro-2-methylphenoxy)acetic acid (MCPA) (97%), and from Avantor: methanol (99.8%), bromophenol blue (100%), $Na_2HPO_4 \times H_2O$, KH_2PO_4, NaCl, NH_4Cl,toluene (99.5%), chloroform (98%), hexane (99%), acetone (99%), NaOH (98%). MCPA was purified by dissolution in toluene, addition of activated carbon, filtration to remove the impurities and crystallized from cold toluene.

Synthesis of herbicidal ionic liquids

The synthesis and characterization of herbicidal ionic liquids were carried out according to previous protocols (Pernak, et al., 2011) and described in detail in the Supplementary Materials (Section 1.1 and 1.2). The purity of the obtained herbicidal ionic liquids was evaluated based on the extractive titration method (Supplementary Materials, Section 1.2). ^{1}H NMR spectra were recorded using a Varian VNMR-S spectrometer operating at 400 MHz with tetramethylsilane as the internal standard. ^{13}C NMR spectra were obtained using the same instrument at 100 MHz. CHN elemental analyses were performed at Adam Mickiewicz University, Poznan. The results of NMR and CHN analyses were presented in the Supplementary Materials (Section 1.3).

Evaluation of electrochemical reactions parameters

The electrochemical kinetics studies were conducted in a three-electrode cell with glassy carbon working electrode (diameter of 3mm, produced by BASI), platinum counter electrode and saturated calomel electrode (SCE) as a reference in the glass vessel (20 cm^3). The working electrode was polished before each measurement. Mineral medium was used as the support electrolyte - phosphorous buffer with addition of chloride anions (composition in

g dm^{-3}: $Na_2HPO_4 \times H_2O$ 7.0; KH_2PO_4 2.8; NaCl 0.5; NH_4Cl 1.0). The concentration of the analysed compounds was equal to 1mM per litre of support electrolyte.

Cyclic voltammetry methods with various scan rates (from 5 mVs^{-1} to 400 mVs^{-1}) were used to determine the charge transfer coefficient, formal potential of reaction, diffusion coefficient, surface concentration of electroactive species and heterogeneous reaction rate constant. Each measurement was repeated three times and standard errors were calculated.

Electrochemical pre-treatment process

Each studied herbicidal ionic liquid (100 mg) was dissolved in 1 dm^3 of the described support electrolyte (mineral medium) and was subjected to the electrochemical oxidation process. The process was conducted in a one compartment cell with a volume of 200 cm^3. The stable current mode with current value equal to 5 mA was applied (this value was experimentally established during previous studies described in Pęziak-Kowalska et al., 2017). The studies were conducted in three-electrode systems. The commercial carbon felt based on polyacrilonitryle (CARBO-GRAF, Racibórz) was used as working electrode material. The electrode size was equal to 20 x 20 x 5mm and it was equipped with a stainless steel collector wire. A coiled platinum wire was used as the counter electrode and saturated calomel electrode was used as the reference electrode. The processes lasted for 4 hours, the samples were taken after 0.5, 1, 2, 3 and 4 hours.

Biodegradation studies

The biodegradation of the studied HILs was evaluated based on the results of a respirometric study using activated sludge (cell density at approx. 10^6 cells per mL determined with plastic Paddle Tester for aerobic bacteria, Hach, USA). The evolution of CO_2 was measured during 28 days for non-treated and electrochemically-treated solutions of each ILs. Additionally, the dissipation of the studied HILs after 28 days was also assessed by establishing the BOD_5/COD ratio. The samples with electrochemically treated HILs solutions were collected after 3 hours of the electrochemical oxidation processes. Samples without HILs were used as biotic controls, whereas samples not inoculated with activated sludge were used as abiotic controls. The CO_2 evolution was determined according to a previously described procedure (Borkowski et al., 2016).

Chemical and Biochemical Oxygen Demand

The Chemical Oxygen Demand (COD) and Biochemical Oxygen Demand (BOD_5) values were evaluated for samples before and after 0.5, 1, 2, 3 and 4 hours of the electrochemical process. The COD parameter was determined by using Nanocolor® COD 600 cuvette tests (Macherey-Nagel, Germany) calibrated with a spectrophotometer (Rayleigh, China) at 620 nm wave length. BOD_5 was measured according to a previously described procedure (Pęziak-Kowalska et al., 2017).

Statistical analysis

All experiments were carried out in triplicates. Each error margin range represents standard errors of the mean (SEM). The SEM values were calculated according to Eq. (2). The calculations were carried out using Statistica 6.0.

Calculation of SEM values:

$SEM = \frac{s}{n^{0.5}}$ (2)

where:

SEM - standard error of the mean,

S - sample standard deviation,

N- number of samples.

3. Results

Synthesis

In the first step, the precursors of HILs (dialkyldimethylammonium bromides) were obtained by the Menschutkin reaction. In the second step of the synthetic process, dialkyldimethylammonium ionic liquids with the MCPA anion were prepared by a metathesis reaction. All the studied HILs are new compounds with the exception of didecyldimethylammonium (4-chloro-2-methylphenoxy)acetate, which was synthesized previously (Pernak, et al., 2011).

The structures of the synthesized dialkyldimethylammonium ionic liquids with the MCPA anion, their purities, yields and states were presented in Table 1.

Table 1. Dialkyldimethylammonium ILs with the MCPA anion

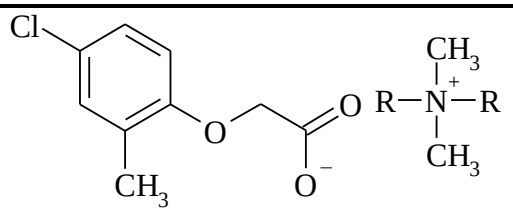

R	Abbreviation of IL	Purity [%]	Yield [%]	State at 25 °C
C_8H_{17}	$[C_8C_8C_1C_1N][MCPA]$	98.0	81	liquid
$C_{10}H_{21}$	$[C_{10}C_{10}C_1C_1N][MCPA]$	99.5	95	liquid
$C_{12}H_{25}$	$[C_{12}C_{12}C_1C_1N][MCPA]$	99.0	93	liquid
$C_{14}H_{29}$	$[C_{14}C_{14}C_1C_1N][MCPA]$	98.5	89	grease
$C_{16}H_{33}$	$[C_{16}C_{16}C_1C_1N][MCPA]$	96.5	89	solid (m. p. 32.5-35.4 °C)
$C_{18}H_{37}$	$[C_{18}C_{18}C_1C_1N][MCPA]$	95.0	94	solid (m. p. 43.5-44.4 °C)

m. p. – melting point

Electrochemical behaviour of HILs

The electrochemical behaviour of HILs was studied using cyclic voltammetry (Fig. 1). The obtained results indicated that the CV curve was similar for all studied compounds. Well-defined anodic peaks were observed at approx. 1.2V/SCE, which were attributed to the oxidation of the studied HILs. These results revealed that the processes were completely irreversible. The observed similarity may suggest that the chain length of the alkyl substituent in the cation did not influence the electrochemical behaviour of HILs.

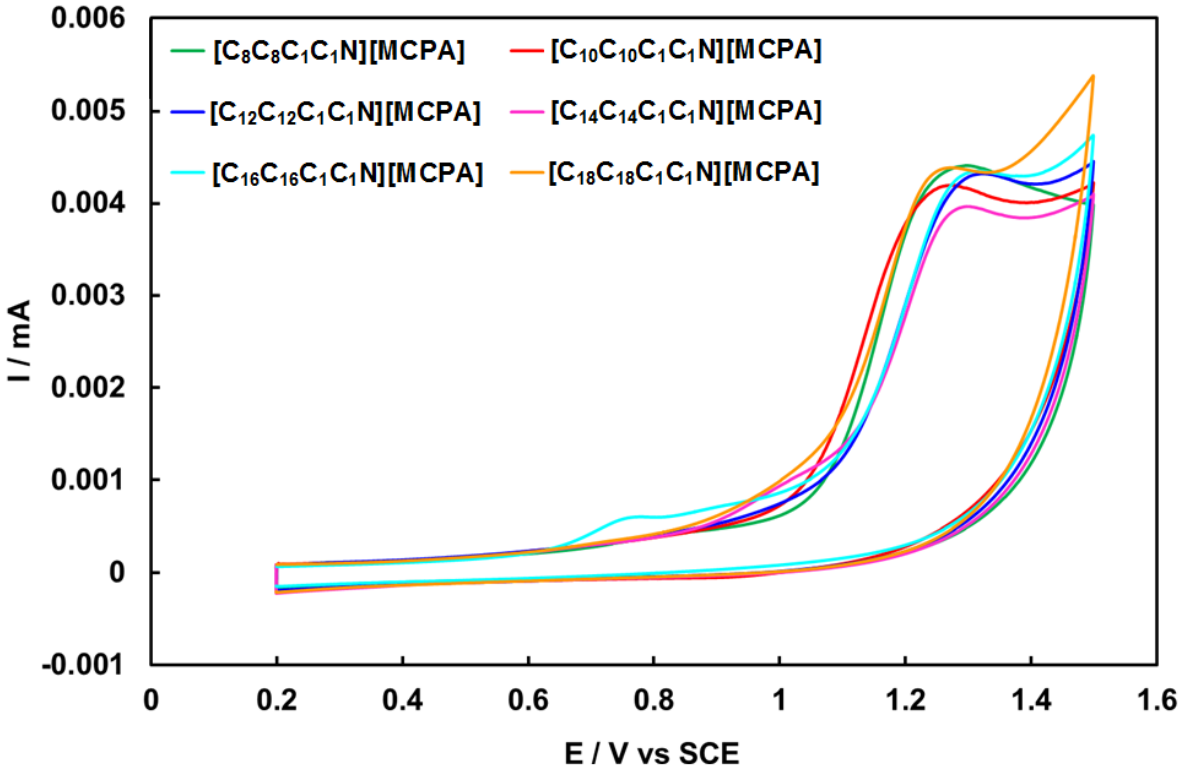

Fig.1. The electrochemical behaviour of tested HILs measured by cyclic voltammetry with a glassy carbon electrode (S = 7.07 mm^2) as working electrode, a Pt counter electrode and SCE as reference electrode, r =10 mVs^{-1}, under room temperature.

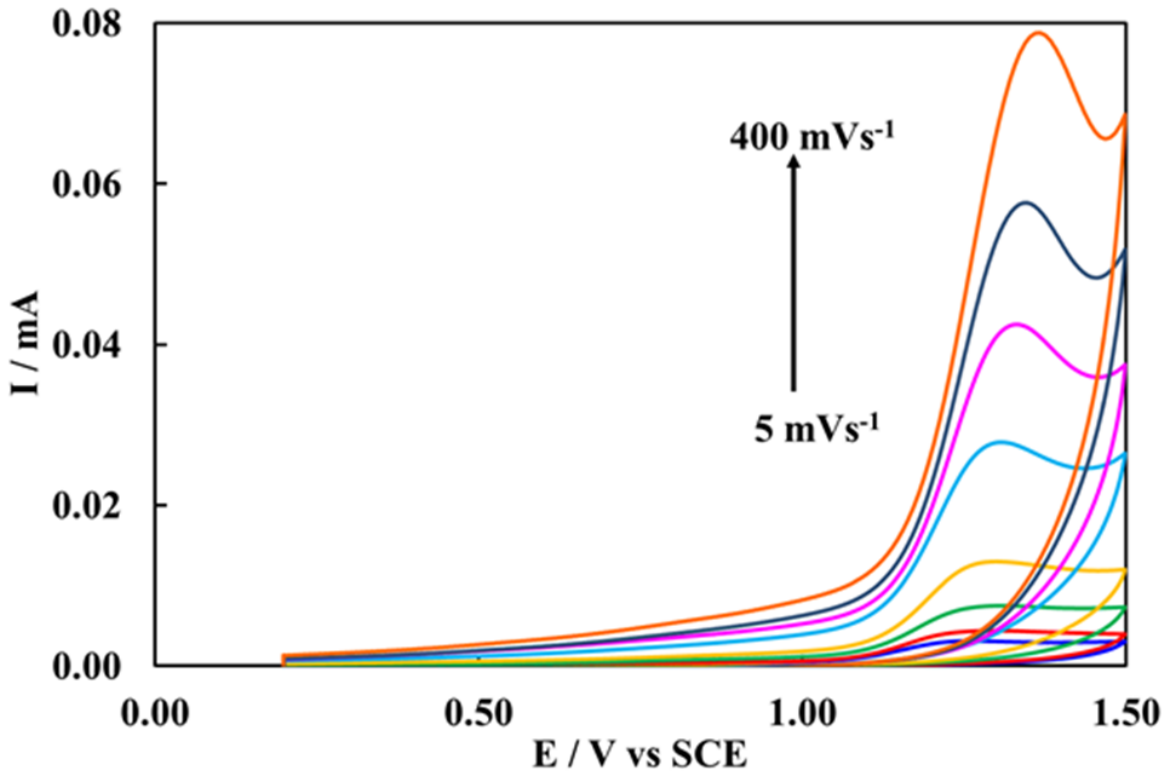

Fig. 2. Cyclic voltammetry responses of 1 mM [$C_8C_8C_1C_1N$][MCPA] at scan rates ranging from 5 to 400 mVs^{-1} with a glassy carbon electrode (S = 7.07 mm^2) as working electrode, a Pt counter electrode and SCE as reference electrode, r =10 mVs^{-1}, under room temperature.

Effect of scan rates

In order to better understand the nature of the HILs oxidation processes, the kinetic parameters of electrode reactions were determined based on CV studies at various scan rates from 5 to 400 mVs^{-1}. The effects of scan rate on the peak potentials and maximal peak current were investigated. Based on these results, the kinetic parameters such as formal potential, electron transfer coefficient and heterogeneous rate constant may be calculated. The obtained dependencies for [$C_8C_8C_1C_1N$][MCPA] as a model HIL were presented in Fig. 2, whereas the data for the remaining HILs may be found in Supplementary Materials (Section 2.1).

All electrochemical processes performed in aqueous systems are limited by adsorption of electroactive species on the electrode surfaces. Moreover, the slop of linear relation between the logarithm of peak current and the logarithm of scan rate was equal to 0.7 for all tested systems (Fig. 3a). This value is higher compared to a typical diffusion-controlled reaction (0.5) however it is also lower than 1, which is characteristic for completely adsorption-controlled processes. These results suggest that the studied electrochemical processes were “mixed” diffusion-adsorption controlled processes (Gosser, 1993).

The dependence between the maximum current of the anodic peak and the square root of scan rate was linear (Fig. 3b) and could be described by equitation 1. This allows for calculation of the diffusion coefficient.

$$I_p = 2{,}99 \times 10^5 \alpha^{1/2} n^{3/2} A C D^{1/2} v^{1/2} \quad (1)$$

where: Ip is the maximum current of anodic peak A, α is the transfer coefficient, n is the number of exchange electrons, A is the area of the electrode [cm^2], C is the bulk concentration in [mol cm^{-3}], D is the diffusion coefficient [cm^2 s^{-1}], ν is the scan rate in [Vs^{-1}] (Zoski, 2007).

In our previous studies, we noticed that the MCPA anion of HILs was generally oxidised during the direct electrochemical reaction (Pęziak-Kowalska et al., 2017). In this case, an attempt to further calculate the exchange of two electrons between electrode surface and MCPA anion in the first step of electrochemical oxidation was made. This assumption was based on the literature data regarding the electrochemical oxidation of phenoxyacetic acids (Fontmorin et al., 2015).

The transfer coefficient α was evaluated according to equation 2:

$$\alpha = \frac{47.7}{E_p - E_{p/2}} mV \quad (2)$$

where: $E_{p/2}$ is the potential at which the current reaches half of the peak value [mV] (Bard and Faulkner, 2004). The transfer coefficients ranged from 0.351 to 0.405 (Table 2), which are typical values for irreversible reactions.

The heterogeneous constant rates of the studied reactions $k^0_{25°C}$ were calculated based on the Velasco equation for irreversible reactions (equation 3) as follows:

$$k^0_{25°C} = 1.11 D^{1/2} \left(E_p - E_{p/2}\right)^{-1/2} \nu^{1/2} \quad (3)$$

where: E_p is the peak potential [mV], $E_{p/2}$ is the potential at which the current reaches half of the peak value [mV], D is the diffusion coefficient [cm^2 s^{-1}], ν is the scan rate [V s^{-1}] (Velasco, 1997).

The surface concentration of electroactive species (Γ) was estimated based on the linear relation between maximal anodic peak current and scan rate (Fig. 3c) as described by equitation 4:

$$I_p = \frac{\alpha n^2 F^2 A \Gamma \nu}{2.718 RT} \quad (4)$$

where: I_p is the maximum current of anodic peak A, n is the number of exchange electrons, F is the Faraday constant [C·mol^{-1}], A is the area of the electrode in [cm^2], ν is the scan rate in [V s^{-1}], R is the gaseous constant [J·$K^{-1}mol^{-1}$], T is the temperature [K] (Sharp et al., 1979).

The heterogeneous constant rates, diffusion coefficients and surface concentrations of electroactive species were collected in Table 2. A similar trend may be observed for all parameters. The values decreased from [$C_8C_8C_1C_1N$][MCPA] to [$C_{12}C_{12}C_1C_1N$][MCPA], dramatically increased in case of [$C_{14}C_{14}C_1C_1N$][MCPA] and decreased again for HILs with longer chains.

Moreover, the formal potentials of these electrochemical reactions were evaluated based on the dependence between the potential and scan rate as the incept of this function (Bard and Faulkner, 2004). The regression equations were presented in Fig.3d. The formal potential values were collected in Table 2. The formal potential was similar for all of the

studied substances and ranged from 1.286 V for [$C_{12}C_{12}C_1C_1N$][MCPA] to 1.323 V for [$C_{18}C_{18}C_1C_1N$][MCPA].

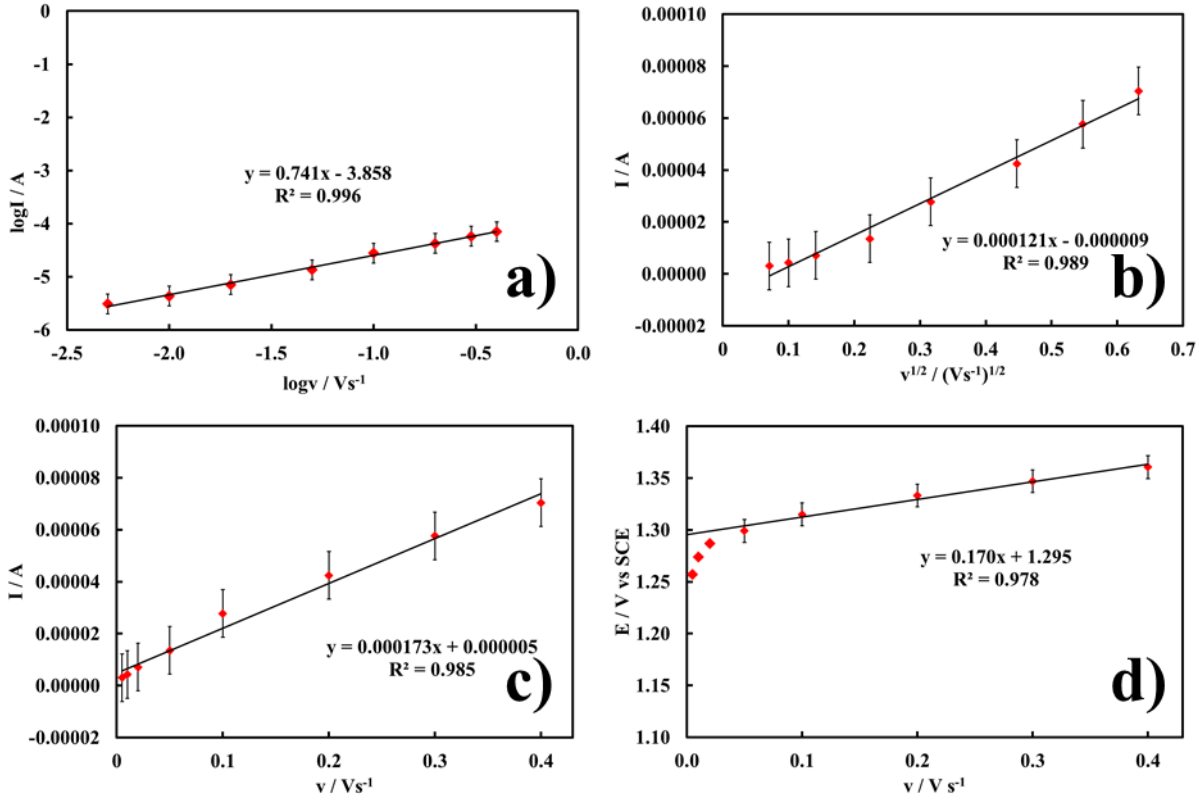

Fig. 3. The dependence between the potential and scan rate obtained for [$C_8C_8C_1C_1N$][MCPA] which present a) peak current logarithm; b) maximal peak current; c) maximal peak current and d) oxidation potential versus scan rate.

Table 2. Summary of the kinetics and hydrodynamic parameters

Substance	Transfer coefficient α	Formal potential [V]	Diffusion coefficient [$10^{-6}cm^2s^{-1}$]	Surface concentration of electroactive species [$10^{-9}molcm^{-2}$]	Heterogeneous rate constant [$10^{-3}cms^{-1}$]
[$C_8C_8C_1C_1N$][MCPA]	0.351	1.295	11.170	1.207	3.96
[$C_{10}C_{10}C_1C_1N$][MCPA]	0.367	1.291	9.126	1.086	3.65
[$C_{12}C_{12}C_1C_1N$][MCPA]	0.393	1.286	5.626	0.818	3.00
[$C_{14}C_{14}C_1C_1N$][MCPA]	0.405	1.298	9.633	1.049	3.92
[$C_{16}C_{16}C_1C_1N$][MCPA]	0.398	1.301	6.748	0.905	3.63
[$C_{18}C_{18}C_1C_1N$][MCPA]	0.386	1.323	5.483	0.821	2.65

Efficiency of electrochemical process

The electrochemical oxidation efficiency of the studied HILs was presented in Fig. 4. In case of the majority of treated solutions, the plateau was achieved after 1 hour.

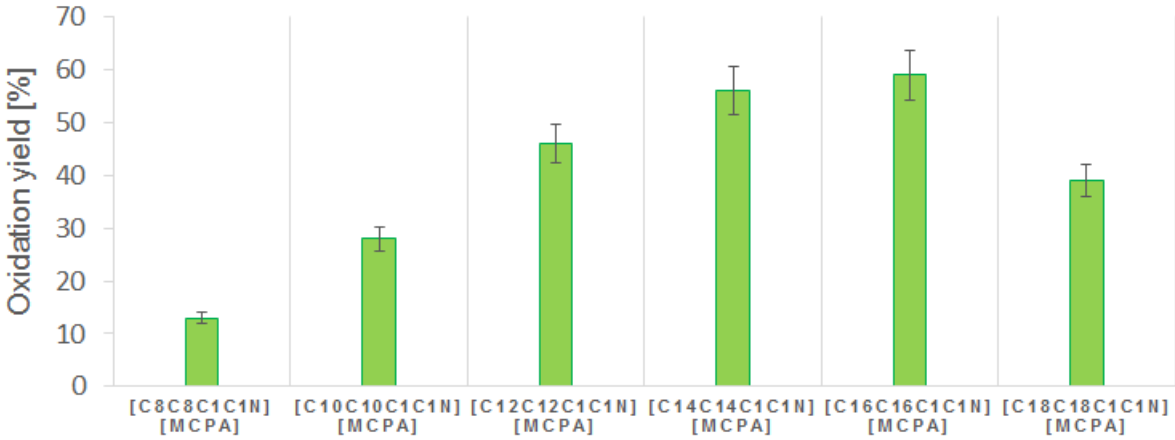

Fig. 4. The oxidation efficiency of HILs solution after 3 hours of electrochemical oxidation process.

In general, the study of electrochemical oxidation of the tested HILs indicated that the efficiency of the process depended on the chain length. The highest oxidation efficiency was observed for [$C_{12}C_{12}C_1C_1N$][MCPA], [$C_{14}C_{14}C_1C_1N$][MCPA] and [$C_{16}C_{16}C_1C_1N$][MCPA] and reached approx. 60% after 4 hours in case of the former, and 3 hours in case of the two latter, respectively. The electrolysis of [$C_8C_8C_1C_1N$][MCPA] was characterized by the lowest efficiency. A detailed characterization of the oxidation process was presented in Supplementary Materials (Section 2.3). The window of maximum efficiency was observed in case of HILs comprising C12-C16 alkyl chains in the cations, whereas the oxidation rate of HILs with shorter or longer substituents was notably lower.

Biodegradation study

Biodegradation of HILs was evaluated before and after the electrochemical pre-treatment. The evaluation of biodegradation efficiency based on CO_2 evolution after 28 days (corrected for biotic control) was presented in Table 3 (the BOD5/COD ratios were presented in Table S1 in the SI).

In case of the majority of the tested HILs, the biodegradation efficiency after 28 days did not exceed 50%. On the other hand, each of the HILs pre-treated with electrochemical oxidation was biodegraded to some extent (biodegradation efficiency ≥ 25%), whereas the non-treated control samples were characterized by limited susceptibility to biodegradation (biodegradation efficiency < 10%). In this case, the alkyl chain length of the substituent also influenced the obtained results. The highest mineralization efficiency in case of

electrochemically pre-treated HILs was observed in case of [$C_{14}C_{14}C_1C_1N$][MCPA] (57%), whereas the lowest value was reached in case of [$C_8C_8C_1C_1N$][MCPA] (28%). A similar tendency was observed in case of non-treated control samples.

Table 3. The biodegradation efficiency of non-treated and electrochemically-treated HILs after 28 days.

	Biodegradation efficiency [%]
Abiotic control	0 ± 1
Non-treated [$C_8C_8C_1C_1N$][MCPA]	0 ± 0
Electrochemically treated [$C_8C_8C_1C_1N$][MCPA]	28 ± 4
Abiotic control	0 ± 0
Non-treated [$C_{10}C_{10}C_1C_1N$][MCPA]	2 ± 1
Electrochemically treated [$C_{10}C_{10}C_1C_1N$][MCPA]	31 ± 7
Abiotic control	0 ± 0
Non-treated [$C_{12}C_{12}C_1C_1N$][MCPA]	5 ± 1
Electrochemically treated [$C_{12}C_{12}C_1C_1N$][MCPA]	37 ± 6
Abiotic control	0 ± 0
Non-treated [$C_{14}C_{14}C_1C_1N$][MCPA]	8 ± 4
Electrochemically treated [$C_{14}C_{14}C_1C_1N$][MCPA]	57 ± 10
Abiotic control	0 ± 1
Non-treated [$C_{16}C_{16}C_1C_1N$][MCPA]	8 ± 3
Electrochemically treated [$C_{16}C_{16}C_1C_1N$][MCPA]	57 ± 8
Abiotic control	0 ± 3
Non-treated [$C_{18}C_{18}C_1C_1N$][MCPA]	1 ± 2
Electrochemically treated [$C_{18}C_{18}C_1C_1N$][MCPA]	36 ± 5

After the biodegradation process, the ratio BOD_5/COD of [$C_{14}C_{14}C_1C_1N$][MCPA] and [$C_{16}C_{16}C_1C_1N$][MCPA] increased from 0.163 and 0.165 to 0.454 and 0.459, respectively (Table S1 in the SI). The samples characterized by values higher than 0.4 may be considered as “readily” biodegradable.

4. Discussion

Herbicidal ionic liquids have been successfully introduced into the commercial market as non-volatile alternatives to classic herbicidal formulations. This group of compounds, introduced for the first time by Pernak et al. (2011), has been constantly expanding and evolving. To date, there are reports regarding HILs which incorporate herbicides such as: 2,4-D (Praczyk et al., 2012; Pernak et al., 2012), MCPA (Pernak et al., 2011), MCPP (Piotrowska et al., 2017), 4-CPA (Syguda et al., 2016), MCPB (Pernak et al., 2016), 2,4-DP (Niemczak et al., 2017a), dicamba (Cojocaru et al., 2013), glyphosate (Pernak et al., 2013a), metsulfuron-

methyl (Pernak et al., 2015a), fomesafen (Ding et al., 2014), clopyralid (Zhu et al., 2015), bentazone (Wang et al., 2015), bromoxynil (Tang et al., 2017), pirolam (Tang et al., 2018) and pelargonate (Pernak et al., 2018) as well as double salts (Choudhary et al., 2017). The group is further diversified by the possibility to employ different cations, e.g. imidazolium, piridynium, ammonium (Pernak et al., 2011, 2012), pyrrolidinium (Syguda et al., 2016), betainium (Niemczak et al., 2017b) or esterquats (Pernak et al., 2015b), cationic forms of herbicides - herbicidal esterquats (Syguda et al., 2018), plant growth regulators (Pernak et al., 2013b), or fungicides (Pernak et al., 2014). The structural diversity of HILs, in addition to the fact that they are introduced directly into the environment, imposes the necessity to monitor their environmental impact and develop effective treatment methods.

Recent studies show that the structure of the cation in HILs may influence their toxicity (Piotrowska et al., 2016, 2017). High toxicity may result in a limitation of natural biodegradation processes or their complete inhibition. It was noticed that the surface active properties of cations in ionic liquids may impact their toxicity and biodegradability by microbial communities from different environmental niches (Ławniczak et al., 2015). The obtained results indicated that the biodegradability of MCPA is generally low (2-25%) and it was further decreased in case of morpholinium HILs (0-7%).

Furthermore, even the introduction of ILs characterized by low toxicity is not necessarily associated with their rapid biodegradation (Sydow et al., 2015). This was observed in case of oligomeric HILs during field trials (Ławniczak et al., 2016). Although the studied HILs did not have a significant impact on the biodiversity of soil microbiota, they were not readily biodegraded. Hence, there is a need to develop methods which would facilitate the biodegradation processes and enhance their efficiency.

Detailed characterization of the electrochemical processes indicated that direct oxidation at the carbon electrode, with the exchange of two electrons as the first step, was the main mechanism of degradation at this stage. Further studies revealed a linear relation between the peak current and square root of scan rate, the logarithm of peak current and logarithm of scan rate as well as the shift of potential towards more positive values with increased of scan rate for all studied HILs. On this basis, it can be assumed that the first step was associated with the irreversible electrochemical reactions, whereas the second step may be a result of irreversible follow-up reaction with e.g. hydroxyl radicals (Zoski, 2007; Bard and Faulkner, 2004; Velasco, 1997).

The formal potentials of all studied HILs during the electrochemical oxidation reactions were similar (approx. 1.3 V) and characteristic for the oxidation potential of

phenoxyacetic acid family (Fontmorin et al., 2013). As previously mentioned, it may be assumed that the MCPA anions mainly underwent direct electrochemical reactions at the electrode surface (Pęziak-Kowalska et al., 2017).

The electrochemical oxidation of selected HILs was characterized by mixed diffusion-adsorption control of process. The dependence between the length of cation alkyl chain (n = 8, 10, 12, 14, 16, 18) and parameters such as heterogeneous rate constant, diffusion coefficient and surface concentration of electroactive species was investigated. Based on the previous reports, it may be assumed that the chain length of alkyl substituents and surface active properties of dialkyldimethylammonium HILs have a strong influence on the described electrode reactions. Pernak et al. noticed that the surface tension decreased with the elongation the ammonium chains up to 16 carbons atom with no further effect (Pernak, et al., 2011; Kordala-Markiewicz et al., 2014). Increased wettability of the electrode material facilitates the contact between the HILs and the electrode material. Overall, this leads to a conclusion that the structure of dialkyldimethylammonium HILs and, in consequence, their surface active properties influence both the diffusion and kinetics of electrochemical oxidation processes. Furthermore, the efficiency of electrolysis estimated by COD parameters confirmed a strong relation between the wettability of electrode material and reaction rate.

Similar relations regarding the length of the alkyl side chain in conventional imidazolium ionic liquids and their decomposition were also observed by Siedlecka et al. (2012). It was noticed that the increase of side chain length reduced the decomposition of imidazolium ring during the electrochemical oxidation in a system with the PbO_2 anode. Moreover, a similar dependence was observed in case of a Fenton-like system (Siedlecka and Stepnowski, 2009). On the other hand, the correlation between the degradation effectivity of imidazolium ionic liquids and chain length was not observed during sonification treatment (Li et al., 2007).

To the best of our knowledge, this is the first attempt to evaluate the efficiency of a hybrid electrochemical-biological treatment of herbicidal ionic liquids. The presented mineralization results confirm that electrochemical pre-treatment increased the susceptibility of the studied HILs to subsequent biological degradation by activated sludge. This confirms the assumption that electrochemical AOPs may be suitable as primary treatment of HILs prior to their biodegradation in wastewater treatment plants.

Conclusion

The results showed that the electrochemical pre-treatment had a positive effect on biodegradation of each tested HILs solutions. Moreover, this hybrid system is a promising solution for the removal of various HILs based on MCPA. The length of alkyl substituents in the cation influenced the kinetic and dynamic parameters of electrochemical oxidation process of dialkyldimetylammonium HILs on the carbon electrode. This approach may be an efficient and economically justified compromise for the treatment of recalcitrant environmental pollutants.

Acknowledgments

This work was financed by funds granted by the National Science Centre (Poland) conferred on the basis of the PRELUDIUM grant decision number [DEC-2014/13/N/NZ9/00789] as well as French-Polish bilateral project (PHC POLONIUM, N° 37768XE and 35491/2016).

Appendix A. Supplementary data

Supplementary data related to this article can be found at http://dx.doi.org/.....

References

Annabi, C., Fourcade, F., Soutrel, I., Geneste, F., Floner, D., Bellakhal N., Amrane, A., 2016. Degradation of enoxacin by the electro-Fenton process: optimization, biodegradability improvement and degradation mechanism., J. Environ. Manage. 165, 96-105.

Bard, A.J., Faulkner, L.R., 2004. Electrochemical Methods: Fundamentals and Applications, 2nd ed., Wiley, New York.

Bomgardner, M. M., 2017. Widespread crop damage from dicamba herbicide fuels controversy. Chem. Eng. News 95(33), 27-29.

Borkowski, A. Ławniczak, Ł, Cłapa, T., Narożna, D., Selwet, M., Pęziak, D., Markiewicz, B., Chrzanowski, Ł, 2016. Different antibacterial activity of novel theophylline-based ionic liquids – Growth kinetic and cytotoxicity studies. Ecotox. Environ. Safe. 130, 54-64.

Brillas, E., Sirés, I., Oturan, M.A., 2009. Electro-Fenton process and related electrochemical technologies based on Fenton's reaction chemistry. Chem. Rev. 109, 6570-6631.

Choudhary, H., Pernak, J., Shamshina, J.L., Niemczak, M., Giszter, R., Chrzanowski, Ł., Praczyk, T., Marcinkowska, K., Cojocaru, O.A., Rogers, R.D., 2017. Two herbicides in

a single compound: double salt herbicidal ionic liquids exemplified with glyphosate, Dicamba, and MCPA. ACS Sustain. Chem. Eng. 5, 6261-6273.

Cojocaru, O.A., Shamshina, J.L., Gurau, G., Syguda, A., Praczyk, T., Pernak, J., Rogers, R.D., 2013. Ionic liquid forms of the herbicide dicamba with reduced volatility and increased efficacy. Green Chem. 15, 2110–2120.

Ding, G., Liu, Y., Wang, B., Punyapitak, D., Guo, M., Duan, Y., Li, J., Cao, Y., 2014. Preparation and characterization of fomesafen ionic liquids for reducing the risk to the aquatic environment. New J. Chem. 38, 5590–5596.

Ferrag-Siagh, F., Fourcade, F., Soutrel, I., Aït Amar, H., Djelal, H., Amrane, A., 2014. Electro-Fenton pretreatment for the improvement of tylosin biodegradability. Environ. Sci. Pollut. R. 21, 8534-8542.

Fontmorin, J.M., Huguet, S., Fourcade, F., Geneste, F., Floner, D., Amrane, A., 2012. Electrochemical oxidation of 2,4-dichlorophenoxyacetic acid: analysis of by-products and improvement of the biodegradability. Chem. Eng. J. 195-196, 208-217.

Fontmorin, J.M., Fourcade, F., Geneste, F., Floner, D., Huguet, S., Amrane, A., 2013. Combined process for 2,4-Dichlorophenoxyacetic acid treatment-Coupling of an electrochemical system with a biological treatment. Biochem. Eng. J. 70, 17–22.

Fontmorin, J.M., Fourcade, F., Geneste, F., Soutrel, I., Floner, D., Amrane, A., 2015. Direct electrochemical oxidation of a pesticide, 2,4-dichlorophenoxyacetic acid, at the surface of a graphite felt electrode: Biodegradability improvement, Comptes Rendus Chim. 18, 32–38.

Garcia-Segura, S., . Lima, Á.S., Cavalcanti, E.B., Brillas, E., 2016, Anodic oxidation, electro-Fenton and photoelectro-Fenton degradations of pyridinium- and imidazolium-based ionic liquids in waters using a BDD/air-diffusion cell, Electrochim. Acta. 198, 68–279.

Gosser, D.K., 1993. Cyclic voltammetry: Simulation and analysis of reaction mechanisms, VCH, New York.

Kordala-Markiewicz, R., Rodak, H., Markiewicz, B., Walkiewicz, F., Sznajdrowska, A., Materna, K., Marcinkowska, K., Praczyk, T., Pernak, J., 2014. Phenoxy herbicidal ammonium ionic liquids, Tetrahedron 70, 4784–4789.

Li, X.H., Zhao, J.G., Li, Q.H ., Wang, L.F., Tsang, S.C., 2007. Ultrasonic chemical oxidative degradations of 1,3-dialkylimidazolium ionic liquids and their mechanistic elucidations, Dalt. Trans. 19, 1875–1880.

Ławniczak, Ł., Materna, K., Framski, G., Szulc, A., Syguda, A., 2015. Comparative study on the biodegradability of morpholinium herbicidal ionic liquids., Biodegrad. 26, 327–

340.

Ławniczak, Ł., Syguda, A., Borkowski, A., Cyplik, P., Marcinkowska, K., Wolko, Ł., Praczyk, T., Chrzanowski, Ł., Pernak, J., 2016. Influence of oligomeric herbicidal ionic liquids with MCPA and Dicamba anions on the community structure of autochthonic bacteria present in agricultural soil. Sci. Total Environ. 563–564, 247–255.

Mansour, D., Fourcade, F., Bellakhal, N., Dachraoui, M., Hauchard, D., Amrane, A., 2012. Biodegradability improvement of sulfamethazine solutions by means of electro-Fenton Process. Water Air Soil Pollut. 223, 2023-2034.

Munoz, M., Domínguez, C.M., De Pedro, Z.M.,. Quintanilla, A., Casas, J.A., Rodriguez, J.J., 2015. Ionic liquids breakdown by Fenton oxidation, Catal. Today. 240, 16–21.

Niemczak, M., Biedziak, A., Czerniak, K., Marcinkowska, K., 2017a. Preparation and characterization of new ionic liquid forms of 2,4-DP herbicide, Tetrahedron 73, 7315–7325.

Niemczak, M., Chrzanowski, L., Praczyk, T., Pernak, J., 2017b. Biodegradable herbicidal ionic liquids based on synthetic auxins and analogues of betaine. New J. Chem. 41, 8066-8077.

Oller, I., Malato, S. Sánchez-Pérez, J.A., 2011. Combination of Advanced Oxidation Processes and biological treatments for wastewater decontamination-A review, Sci. Total Environ. 409, 4141–4166.

Pernak, J., Branicka, M., 2004. Synthesis and aqueous ozonation of some pyridinium salts with alkoxymethyl and alkylthiomethyl hydrophobic groups. Ind. Eng. Chem. Res. 43, 1966–1974.

Pernak, J., Syguda, A., Janiszewska, D., Materna, K., Praczyk, T., 2011. Ionic liquids with herbicidal anions. Tetrahedron 67, 4838–4844.

Pernak, J., Syguda, A., Materna, K., Janus, E., Kardasz, P., Praczyk, T., 2012. 2,4-D based herbicidal ionic liquids. Tetrahedron 68, 4267–4273.

Pernak, J., Niemczak, M., Materna, K., Marcinkowska, K., Praczyk, T., 2013. Ionic liquids as herbicides and plant growth regulators, Tetrahedron 69, 4665–4669.

Pernak, J., Niemczak, M., Giszter, R., Shamshina, J.L., Gurau, G., Cojocaru, O.A., Praczyk, T., Marcinkowska, K., Rogers, R.D., 2014a. Glyphosate-based herbicidal ionic liquids with increased efficacy. ACS Sustain. Chem. Eng. 2, 2845–2851.

Pernak, J., Markiewicz, B., Zgoła-Grześkowiak, A., Chrzanowski, Ł., Gwiazdowski, R., Praczyk, T., Marcinkowska, K., 2014b. Ionic liquids with dual pesticidal function. RSC Adv. 4, 39751–39754.

Pernak, J., Niemczak, M., Shamshina, J.L., Gurau, G., Głowacki, G., Praczyk, T., Marcinkowska, K., Rogers, R.D., 2015a. Metsulfuron-Methyl-Based Herbicidal Ionic Liquids. J. Agric. Food Chem. 63, 3357–3366.

Pernak, J., Czerniak, K., Niemczak, M., Chrzanowski Ł., Ławniczak, Ł., Fochtman, P., Marcinkowska, K., Praczyk, T., 2015b. Herbicidal ionic liquids based on esterquats. New J. Chem. 39, 5715–24.

Pernak, J., Niemczak, M., Materna, K., Żelechowski, K., Marcinkowska, K. Praczyk, T., 2016. Synthesis, properties and evaluation of biological activity of herbicidal ionic liquids with 4-(4-chloro-2-methylphenoxy)butanoate anion. RSC Adv. 6, 7330–7338.

Pernak, J., Czerniak,K., Niemczak,M.,. Ławniczak, Ł. Kaczmarek, D.K.,. Borkowski, A., Praczyk, T., 2018. Bioherbicidal Ionic Liquids. ACS Sustain. Chem. Eng. 6, 2741−2750.

Pęziak-Kowalska, D., Fourcade, F., Niemczak, M., Amrane, A,. Chrzanowski, Ł., Lota, G., 2017. Removal of herbicidal ionic liquids by electrochemical advanced oxidation processes combined with biological treatment. Environ. Technol. (United Kingdom) 38, 1093–1099.

Pieczyńska, A., Ofiarska, A., Borzyszkowska, A.F., Białk-Bielińska, A,. Stepnowski, P., Stolte, S., Siedlecka, E.M., 2015. A comparative study of electrochemical degradation of imidazolium and pyridinium ionic liquids: A reaction pathway and ecotoxicity evaluation. Sep. Purif. Technol. 156, 522–534.

Piotrowska, A., Syguda, A., Chrzanowski, Ł.,Heipieper, H.J., 2016. Toxicity of synthetic herbicides containing 2,4-D and MCPA moieties towards *Pseudomonas putida* mt-2 and its response at the level of membrane fatty acid composition. Chemosphere 144, 107–112.

Piotrowska, A., Syguda, A.,Wyrwas, B., Chrzanowski, Ł.,Heipieper, H.J., 2017. Toxicity evaluation of selected ammonium-based ionic liquid forms with MCPP and dicamba moieties on *Pseudomonas putida*.Chemosphere 167, 114–119.

Piotrowska, A., Syguda, A., Wyrwas, B., Chrzanowski, L., Luckenbach, T., Heipieper, H.J., 2018. Effects of ammonium-based ionic liquids and 2,4-dichlorophenol on the phospholipid fatty acid composition of zebrafish embryos. PLoS ONE 13, e0190779.

Praczyk, T., Kardasz, P., Jakubiak, E., Syguda, A., Materna, K., Pernak J., 2012. Herbicidal Ionic Liquids with 2,4-D. Weed Sci. 60, 189–192.

Sharp, M., Petersson, M., Edström, K, 1979. Preliminary determinations of electron transfer kinetics involving ferrocene covalently attached to a platinum surface, J. Electroanal.

Chem. 95, 123–136.

Siedlecka, E.M., Mrozik, W., Kaczyński, Z., Stepnowski, P., 2008. Degradation of 1-butyl-3-methylimidazolium chloride ionic liquid in a Fenton-like system, J. Hazard. Mater. 154, 893–900.

Siedlecka, E.M., Stepnowski, P., 2009. The effect of alkyl chain length on the degradation of alkylimidazolium- and pyridinium-type ionic liquids in a Fenton-like system, Environ. Sci. Pollut. Res. 16, 453–458.

Siedlecka, E.M., Stolte, S., Gołebiowski, M., Nienstedt, A., Stepnowski, P., Thöming, J., 2012. Advanced oxidation process for the removal of ionic liquids from water: The influence of functionalized side chains on the electrochemical degradability of imidazolium cations. Sep. Purif. Technol. 101, 26–33.

Sirés, I., Brillas, E., Oturan, M.A., Rodrigo, M.A., Panizza, M., 2014. Electrochemical advanced oxidation processes: Today and tomorrow. A review. Environ. Sci. Pollut. Res. 21, 8336–8367.

Stepnowski, P., Zaleska, A., 2005. Comparison of different advanced oxidation processes for the degradation of room temperature ionic liquids. J. Photochem. Photobiol. A. 170, 45–50.

Stolte, S., Abdulkarim, S., Blomeyer-Nienstedt, A., 2008. Primary biodegradation of ionic liquid cations, identification of degradation products of 1-methyl-3-octylimidazolium chloride and electrochemical wastewater treatment of poorly biodegradable compounds. Green Chem. 10, 214–224.

Sydow, M., Szczepaniak, Z., Framski, G., Staninska, J.,Owsianiak, M., Szulc, A., Piotrowska-Cyplik, A., Zgoła-Grześkowiak, A., Wyrwas, B., Chrzanowski, Ł., 2015.Persistence of selected ammonium- and phosphonium-based ionic liquids in urban park soil microcosms. Int. Biodeterior. Biodegrad. 103, 91–96.

Syguda, A., Materna, K., Marcinkowska, K., 2016. Pyrrolidinium herbicidal ionic liquids. RSC Adv. 6, 63136–63142.

Syguda, A., Gielnik, A., Borkowski, A., Woźniak-Karczewska, M., Parus, A., Piechalak, A., Olejnik, A., Marecik, R., Ławniczak, Ł., Chrzanowski, Ł., 2018. Esterquat herbicidal ionic liquids (HILs) with two different herbicides: evaluation of activity and phytotoxicity. New J. Chem. 42, 9819–9827.

Tang, G., Liu, Y. Ding, G., Zhang, W., Liang, Y., Fan, C., Dong, H., Yang, J., Kong, D., Cao, Y., 2017. Ionic liquids based on bromoxynil for reducing adverse impacts on the environment and human health. New J. Chem. 41, 8650–8655.

Tang, G., Wang, B., Ding, G., Zhang, W., Liang, Y., Fan, C., Dong, H., Yang, J., Kong, D., Cao, Y.2018. Developing ionic liquid forms of picloram with reduced negative effects on the aquatic environment. Sci. Total Environ. 616–617, 128–134

Velasco, J. G., 1997. Determination of Standard Rate Constants for Electrochemical Irreversible Processes from Linear Sweep Voltammograms. Electroanalysis 9, 880–882.

Wang, B., Ding, G., Zhu, J., Zhang, W., Guo, M., Geng, Q., Guo, D., Cao, Y., 2015. Development of novel ionic liquids based on bentazone. Tetrahedron 71, 7860–7864.

Yahiaoui, I., Yahia, C. L., Madi, K., Aissani-Benissad, F., Fourcade, F., Amrane, A. 2018. The feasibility of combining an electrochemical treatment on a carbon felt electrode and a biological treatment for the degradation of tetracycline and tylosin – application of the experimental design methodology. Sep. Sci. Technol. 53, 337-348.

Zajac, A., Kukawka, R., Pawlowska-Zygarowicz, A., Stolarska, O., Smiglak, M., 2018. Ionic liquids as bioactive chemical tools for use in agriculture and the preservation of agricultural products. Green Chem. 20, 4764-4789.

Zhu, J., Ding, G., Liu, Y., Wang, B., Zhang, W., Guo, M., Geng, Q., Cao,Y., 2015. Ionic liquid forms of clopyralid with increased efficacy against weeds and reduced leaching from soils. Chem. Eng. J. 279, 472–477.

Zoski, C. G., 2007. Handbook of electrochemisry, Elsevier, Amsterdam.

ELECTRONIC SUPPLEMENTARY INFORMATION

Hybrid electrochemical and biological treatment of herbicidal ionic liquids comprising the MCPA anion

Daria Pęziak-Kowalska[1], Anna Syguda[2], Łukasz Ławniczak[2], Andrzej Borkowski[3], Florence Fourcade[4], Hermann J. Heipieper[5], Grzegorz Lota[1], Łukasz Chrzanowski[2,*]

[1]Institute of Chemistry and Technical Electrochemistry, Poznan University of Technology, ul. Bedrychowo 4, 60-965 Poznan, Poland.
[2]Institute of Chemical Technology and Enginering, Poznan University of Technology, ul. Bedrychowo 4, 60-965 Poznan, Poland.
[3]Faculty of Geology, University of Warsaw, Żwirki i Wigury 93, 02-089 Warsaw, Poland.
[4]Université Rennes 1/Ecole Nationale Supérieure de Chimie de Rennes, CNRS, UMR 6226, 11 allées de Beaulieu, CS 50837, 35708 Rennes Cedex 7, France.
[5]Helmholtz Centre for Environmental Research – UFZ, Department of Environmental Biotechnology, Permoserstraße 15, D-04318 Leipzig, Germany.
Corresponding author: lukasz.chrzanowski@put.poznan.pl

1. Synthesis and analysis of ionic liquids

1.1. Synthesis of ionic liquids

I Step: dialkyldimethylammonium bromides: 0.1 mol of 1-bromoalkane (1-bromooctane, 1-bromodecane, 1-bromododecane, 1-bromotetradecane, 1-bromohexadecane or 1-bromooctadecane) was added into a round-bottomed flask equipped with a reflux condenser and magnetic stirrer and contained solution of 0.1 mol adequate alkyldimethylamine (dimethyloctylamine, decyldimethylamine, dodecyldimethylamine, tetradecyldimethylamine, heksadecyldimethylamine or dimethyloctadecylamine) in 20 mL acetone. The reaction mixture was vigorously stirred at boiling temperature under a reflux condenser for 24 h. Afterwards acetone was evaporated and crude product was cooled in the freezer for 24 hours. The precipitate was filtered, washed with hexane and dried at 50 °C under reduced pressure (12 hPa).

II Step: dialkyldimethylammonium ionic liquids with MCPA anion (Scheme 1): 0.011mol of 10 % aqueous solution of sodium hydroxide was added into suspension of 0.01 mol of MCPA in the acid form in 20 mL distilled water. The reaction mixture was mixed and heated at 50 °C until the solution became clear. Afterwards, 0.01 mol of appropriate dialkyldimethylammonium bromide dissolved in water and isopropanol (30 mL water and 30 mL isopropanol) was added and stirred for 20 min at room temperature. The product was extracted from the aqueous phase with 60 mL of chloroform and washed with distilled water until bromide ions were no longer detected using $AgNO_3$. After evaporation of chloroform, the product was dried under reduced pressure (12 hPa) at 60 °C for 24 h.

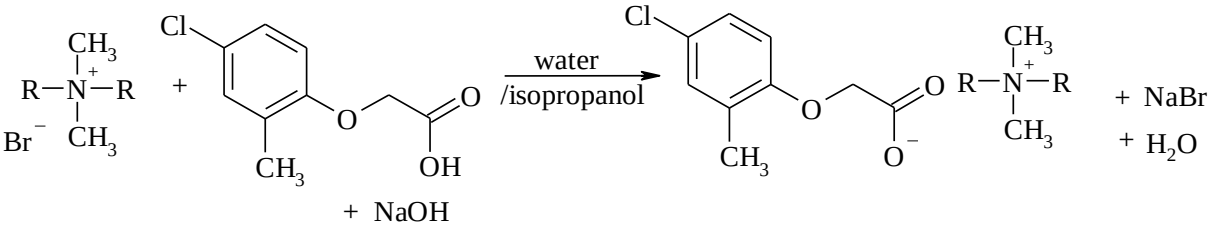

Scheme 1. Synthesis of dialkyldimethylammonium ionic liquids with MCPA anion.

1.2. Quantitative analysis of the dialkyldimethylammonium ionic liquid with MCPA anion

The concentration of dialkyldimethylammonium (4-chloro-2-methylphenoxy)acetate (purity) was determined according to the extractive titration method (Cross, 1965; Wang and Weng, 1995) in alkaline water-chloroform system using sodium tetraphenylborate as the titrant and the bromophenol blue in the acid form (0.2% in methanol) as the indicator. The indicator is soluble in water and insoluble in chloroform, but can be extracted into chloroform as blue ion complex with dialkyldimethylammoniumcation. When the dialkyldimethylammoniumsalt as the complex with bromophenol blue is titrated with sodium tetraphenylborate solution, the dialkyldimethylammoniumtetraphenylborate is formed. Exchanged bromophenol blue anion with sodium cation is not soluble in chloroform and turns on to the water phase to give purple color. The end point is marked by the appearance of purple color of indicator in alkaline aqueous layer after decomposition of the chloroform-soluble blue complex and then the chloroform layer turns from blue to colorless. In a Erlenmeyer flask with a glass stopper 0.1 ± 0.0001 g of the sample was placed and blended with 30 mL of chloroform, 10 mL of NaOH water solution (1 mol/L) and six drops of indicator. The resulting biphasic system was titrated with 0.01 mol/L of sodium

tetraphenylborate solution. After addition of a titrant increment, the flask was stopped and the sample was stirred vigorously for is essential to avoid over titration.

The purity as the concentration of dialkyldimethylammoniumionic liquid was calculated using equation (1):

$$X = \frac{C_{TFB} \cdot V_{TFB} \cdot M}{1000 \cdot m_s} \cdot 100\,[\%] \quad (1)$$

where:

X – concentration of dialkyldimethylammonium(4-chloro-2-methylphenoxy)acetate [%]

C_{TFB} – concentration of sodium tetraphenylborate [mol/L]

V_{TFB} – volume of the titrant solution [mL]

M – molecular weight of analyzed compound [g/mol]

m_s – mass of the analyzed sample [g]

1.3. NMR spectra and elemental analyses

The following abbreviations were used to explain the multiplicities:
s = singlet, d = doublet, dd = doublet of doublets, t = triplet, q = quintet, m = multiplet

Dimethydioctylammonium (4-chloro-2-methylphenoxy)acetate ([$C_8C_8C_1C_1N$][MCPA]) ^{1}H NMR ($CDCl_3$) δ ppm = 0.81 (t, *J* = 6.9 Hz, 6H), 1.18 (m, 20H), 1.49 (q, *J* = 7.8 Hz, 4H), 2.16 (s, 3H), 3.01 (s, 6H), 3.07 (t, *J* = 8.6 Hz, 4H), 4.30 (s, 2H), 6.67 (d, *J* = 8.5 Hz, 1H), 6.96 (dd, $J^{1,2}$= 2.7 Hz, $J^{1,3}$= 8.6 Hz, 1H), 6.97 (d, *J* = 2.4 Hz, 1H); ^{13}C NMR δ ppm = 13.5, 15.9, 22.0, 22.1, 25.7, 28.6, 28.7, 28.9, 31.3, 50.8, 62.6, 68.0, 112.3, 123.6, 125.6, 128.0, 129.4, 155.6, 172.7.Anal. Calcd for $C_{27}H_{48}ClNO_3$: C 68.96, H10.31, N 2.98; Found: C 69.33, H 10.49, N 3.17.

Didecyldimethylammonium (4-chloro-2-methylphenoxy)acetate ([$C_{10}C_{10}C_1C_1N$][MCPA]) ^{1}H NMR ($CDCl_3$) δ ppm = 0.88 (t, *J* = 6.7 Hz, 6H), 1.25 (m, 28H), 1.57 (q, *J* = 6.9 Hz, 4H), 2.24 (s, 3H), 3.12 (s, 6H), 3.21 (t, *J* = 8.5 Hz, 4H), 4.41 (s, 2H), 6.75 (d, *J* = 8.8 Hz, 1H), 7.00 (dd, $J^{1,2}$= 2.6 Hz, $J^{1,3}$= 8.8 Hz, 1H), 7.05 (d, *J* = 2.6 Hz, 1H); ^{13}C NMR δ ppm = 14.0, 16.3, 22.5, 22.52, 26.1, 29.06, 29.12, 29.26, 29.30, 31.7, 51.1, 63.3, 68.4, 112.7, 124.1, 126.0, 128.4, 129.9, 156.1, 173.1. Anal. Calcd for $C_{31}H_{56}ClNO_3$: C 70.75, H10.73, N 2.66; Found: C 70.81, H 10.81, N 2.55.

Didodecyldimethylammonium (4-chloro-2-methylphenoxy)acetate ([$C_{12}C_{12}C_1C_1N$][MCPA]) ^{1}H NMR ($CDCl_3$) δ ppm = 0.88 (t, *J* = 6.7 Hz, 6H), 1.25 (m, 36H), 1.60 (q, *J* = 6.9 Hz, 4H),

2.20 (s, 3H), 3.20 (s, 6H), 3.29 (t, J = 8.5 Hz, 4H), 4.36 (s, 2H), 6.72 (d, J = 8.9 Hz, 1H), 7.00 (dd, $J^{1,2}$= 2.6 Hz, $J^{1,3}$= 8.9 Hz, 1H), 7.03 (d, J = 2.6 Hz, 1H); ^{13}C NMR δ ppm = 13.9, 16.2, 22.5, 22.9, 26.1, 29.1, 29.28, 29.35, 29.46, 29.51, 31.7, 52.8, 63.3, 68.3, 112.7, 124.1, 126.0, 128.3, 129.8, 155.9, 173.3. Anal. Calcd for $C_{35}H_{64}ClNO_3$: C 72.17, H11.10, N 2.41; Found: C 72.53, H 11.15, N 2.36.

Dimethylditetradecylammonium (4-chloro-2-methylphenoxy)acetate ([$C_{14}C_{14}C_1C_1N$][MCPA]) ^{1}H NMR ($CDCl_3$) δ ppm = 0.88 (t, J = 6.7 Hz, 6H), 1.26 (m, 44H), 1.58 (q, J = 6.8 Hz, 4H), 2.23 (s, 3H), 3.07 (s, 6H), 3.14 (t, J = 7.8 Hz, 4H), 4.40 (s, 2H), 6.71 (d, J = 8.5 Hz, 1H), 7.01 (dd, $J^{1,2}$= 2.6 Hz, $J^{1,3}$= 8.5 Hz, 1H), 7.04 (d, J = 2.6 Hz, 1H); ^{13}C NMR δ ppm = 14.0, 16.3, 22.46, 22.54, 26.1, 29.0, 29.22, 29.25, 29.4, 29.5, 29.6, 31.8, 51.1, 63.4, 68.1, 112.7, 124.3, 126.0, 128.5, 129.9, 155.8, 174.2. Anal. Calcd for $C_{39}H_{72}ClNO_3$: C 73.35, H11.39, N 2.19; Found: C 72.99, H 11.51, N 2.05.

Dihexyldimethylammonium (4-chloro-2-methylphenoxy)acetate ([$C_{16}C_{16}C_1C_1N$][MCPA]) ^{1}H NMR ($CDCl_3$) δ ppm = 0.88 (t, J = 6.7 Hz, 6H), 1.26 (m, 52H), 1.59 (q, J = 6.9 Hz, 4H), 2.24 (s, 3H), 3.23 (s, 6H), 3.30 (t, J = 8.5 Hz, 4H), 4.41 (s, 2H), 6.76 (d, J = 8.8 Hz, 1H), 6.99 (dd, $J^{1,2}$= 2.6 Hz, $J^{1,3}$= 8.8 Hz, 1H), 7.04 (d, J = 2.6 Hz, 1H); ^{13}C NMR δ ppm = 14.0, 16.3, 22.5, 26.1, 29.1, 29.21, 29.22, 29.34, 29.45, 29.51, 29.55, 31.8, 50.8, 63.3, 68.8, 112.7, 123.8, 125.9, 128.3, 129.8, 156.3, 172.8. Anal. Calcd for $C_{44}H_{80}ClNO_3$: C 74.78, H11.43, N 1.98; Found: C 75.12, H 11.15, N 2.07.

Dimethydioctadecylammonium (4-chloro-2-methylphenoxy)acetate ([$C_{18}C_{18}C_1C_1N$][MCPA]) ^{1}H NMR ($CDCl_3$) δ ppm = 0.88 (t, J = 6.8 Hz, 6H), 1.26 (m, 60H), 1.63 (q, J = 6.9 Hz, 4H), 2.21 (s, 3H), 3.28 (s, 6H), 3.37 (t, J = 8.3 Hz, 4H), 4.41 (s, 2H), 6.76 (d, J = 8.8 Hz, 1H), 7.03 (dd, $J^{1,2}$= 2.6 Hz, $J^{1,3}$= 8.8 Hz, 1H), 7.10 (d, J = 2.6 Hz, 1H); ^{13}C NMR δ ppm = 14.0, 16.4, 22.6, 26.1, 29.1, 29.2, 29.3, 29.49, 29.53, 29.6, 31.8, 51.1, 63.4, 68.7, 112.7, 124.0, 126.0, 128.3, 129.8, 156.2, 173.1. Anal. Calcd for $C_{48}H_{88}ClNO_3$: C 75.57, H11.65, N 1.84; Found: C 75.09, H 11.89, N 1.77.

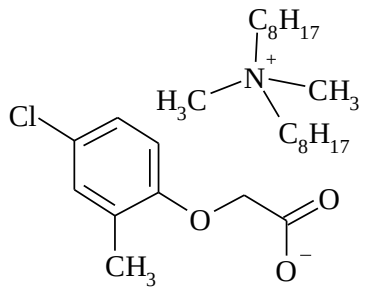

[$C_8C_8C_1C_1N$][MCPA] *Dimethydioctylammonium (4-chloro-2-methylphenoxy)acetate*

^{1}H NMR ($CDCl_3$) δ ppm = 0.81 (t, *J* = 6.9 Hz, 6H), 1.18 (m, 20H), 1.49 (q, *J* = 7.8 Hz, 4H), 2.16 (s, 3H), 3.01 (s, 6H), 3.07 (t, *J* = 8.6 Hz, 4H), 4.12 (H_2O), 4.30 (s, 2H), 6.67 (d, *J* = 8.5 Hz, 1H), 6.96 (dd, $J^{1,2}$= 2.7 Hz, $J^{1,3}$= 8.6 Hz, 1H), 6.97 (d, *J* = 2.4 Hz, 1H).

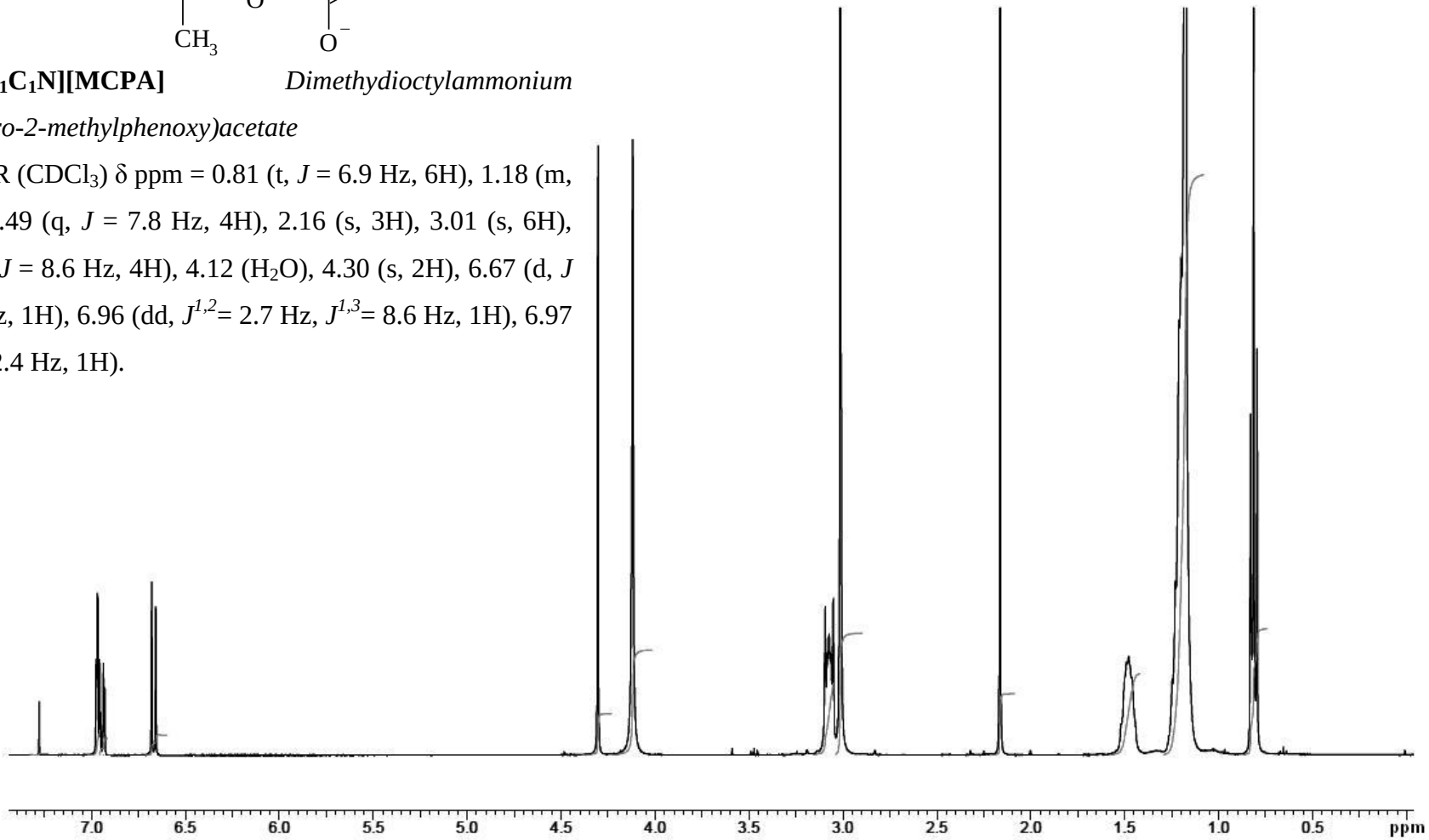

Fig. S1. ^{1}H NMR spectrum of [$C_8C_8C_1C_1N$][MCPA].

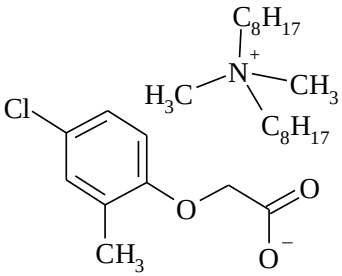

[$C_8C_8C_1C_1N$][MCPA] *Dimethydioctylammonium (4-chloro-2-methylphenoxy)acetate*

^{13}C NMR ($CDCl_3$) δ ppm = 14.0, 16.3, 22.5, 22.52, 26.1, 29.06, 29.12, 29.26, 29.30, 31.7, 51.1, 63.3, 68.4, 112.7, 124.1, 126.0, 128.4, 129.9, 156.1, 173.1.

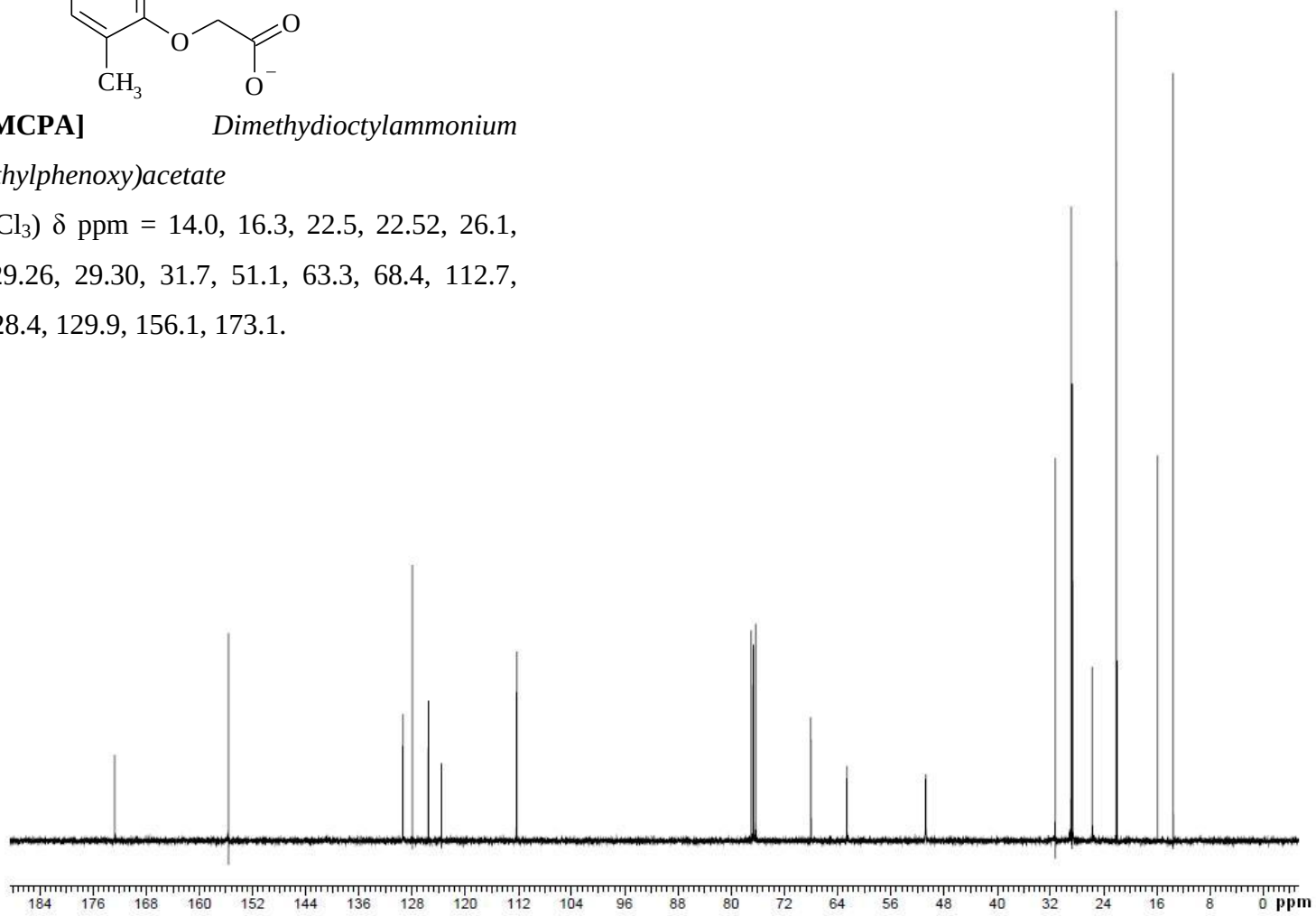

Fig. S2. ^{13}C NMR spectrum of [$C_8C_8C_1C_1N$][MCPA].

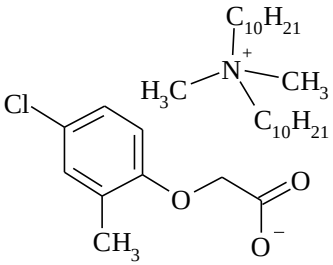

[$C_{10}C_{10}C_1C_1N$][MCPA] *Didecyldimethylammonium (4-chloro-2-methylphenoxy)acetate*

^{1}H NMR ($CDCl_3$) δ ppm = 0.88 (t, *J* = 6.7 Hz, 6H), 1.25 (m, 28H), 1.57 (q, *J* = 6.9 Hz, 4H), 2.24 (s, 3H), 3.12 (s, 6H), 3.21 (t, *J* = 8.5 Hz, 4H), 4.19 (H_2O), 4.41 (s, 2H), 6.75 (d, *J* = 8.8 Hz, 1H), 7.00 (dd, $J^{1,2}$= 2.6 Hz, $J^{1,3}$= 8.8 Hz, 1H), 7.05 (d, *J* = 2.6 Hz, 1H).

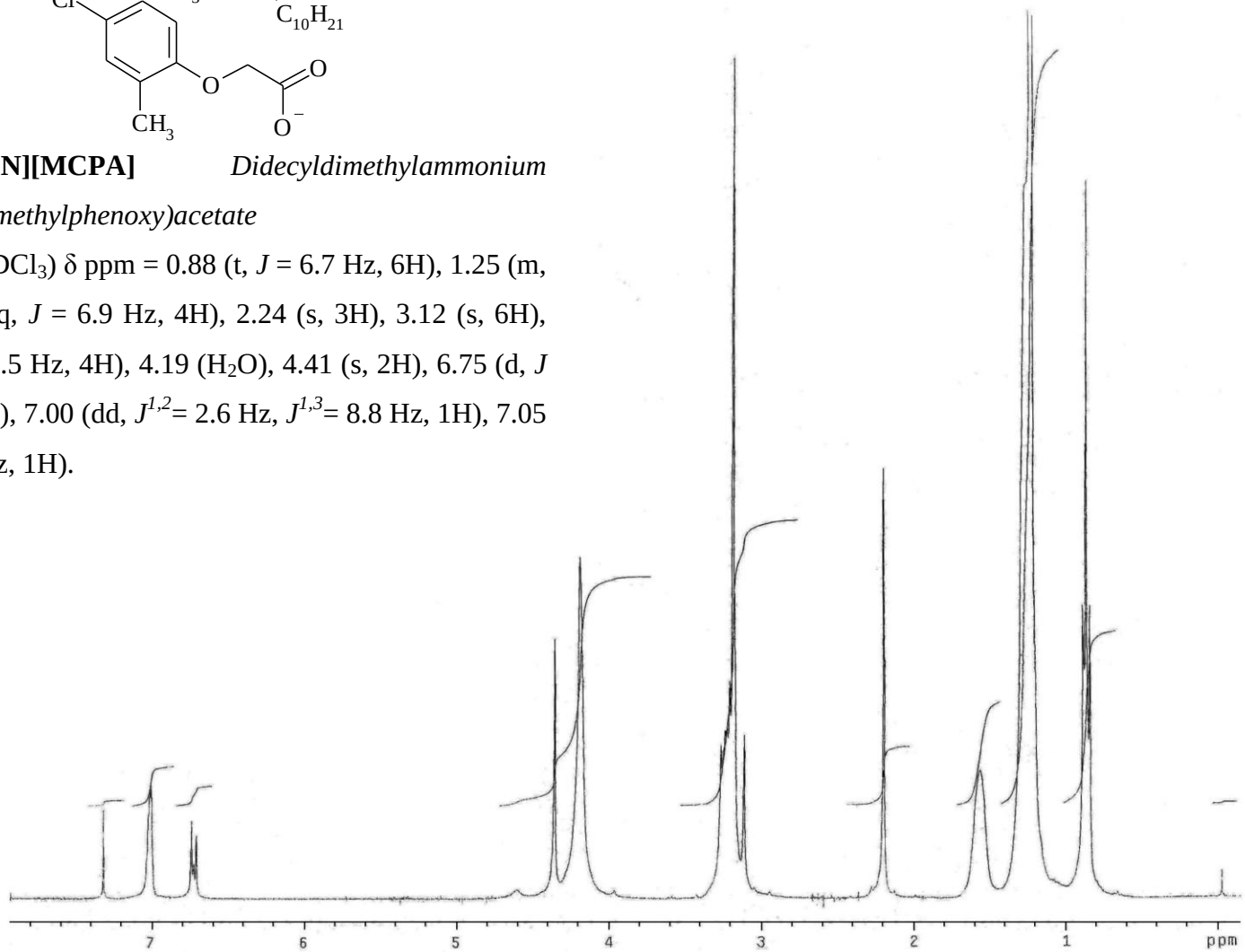

Fig. S3. ^{1}H NMR spectrum of [$C_{10}C_{10}C_1C_1N$][MCPA].

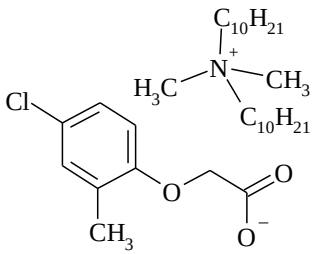

[$C_{10}C_{10}C_1C_1N$][MCPA] *Didecyldimethylammonium (4-chloro-2-methylphenoxy)acetate*

^{13}C NMR ($CDCl_3$) δ ppm = 14.0, 16.3, 22.5, 22.52, 26.1, 29.06, 29.12, 29.26, 29.30, 31.7, 51.1, 63.3, 68.4, 112.7, 124.1, 126.0, 128.4, 129.9, 156.1, 173.1.

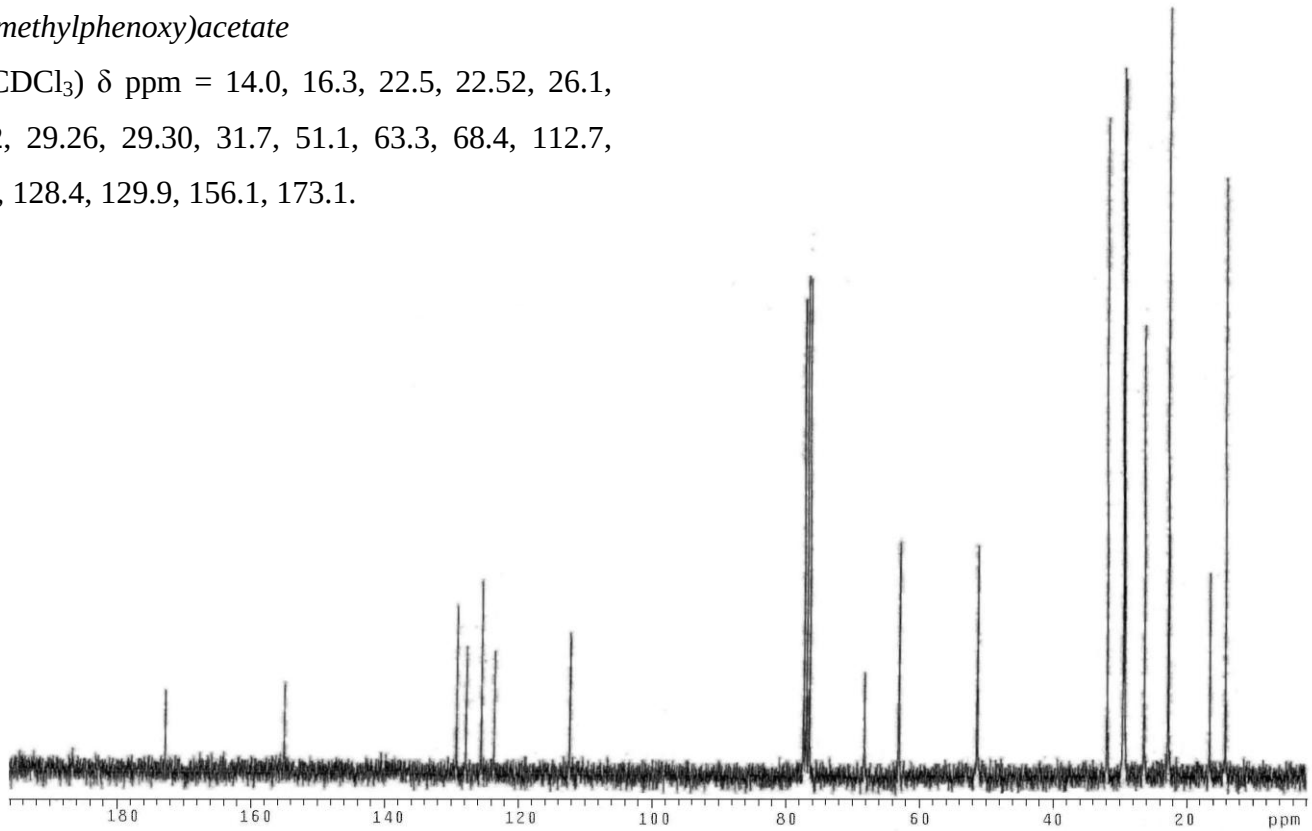

Fig. S4. ^{13}C NMR spectrum of [$C_{10}C_{10}C_1C_1N$][MCPA].

[$C_{12}C_{12}C_1C_1N$][MCPA] *Didodecyldimethylammonium (4-chloro-2-methylphenoxy)acetate*

^{1}H NMR ($CDCl_3$) δ ppm = ^{1}H NMR ($CDCl_3$) δ ppm = 0.88 (t, J = 6.7 Hz, 6H), 1.25 (m, 36H), 1.60 (q, J = 6.9 Hz, 4H), 2.20 (s, 3H), 3.20 (s, 6H), 3.29 (t, J = 8.5 Hz, 4H), 4.36 (H_2O), 4.36 (s, 2H), 6.72 (d, J = 8.9 Hz, 1H), 7.00 (dd, $J^{1,2}$= 2.6 Hz, $J^{1,3}$= 8.9 Hz, 1H), 7.03 (d, J = 2.6 Hz, 1H).

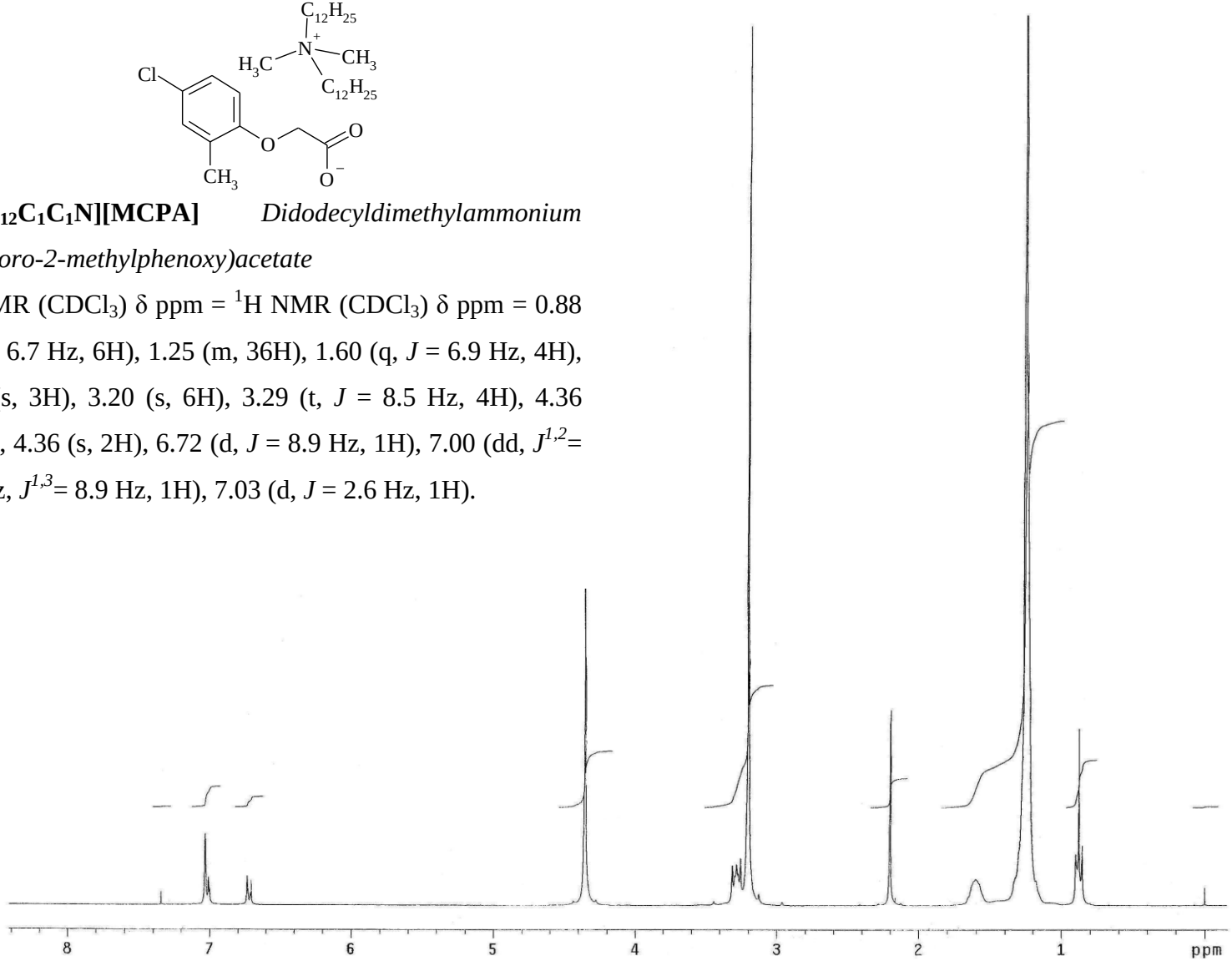

Fig. S5. ^{1}H NMR spectrum of [$C_{12}C_{12}C_1C_1N$][MCPA].

[$C_{12}C_{12}C_1C_1N$][MCPA] *Didodecyldimethylammonium (4-chloro-2-methylphenoxy)acetate*

^{13}C NMR ($CDCl_3$) δ ppm = 13.9, 16.2, 22.5, 22.9, 26.1, 29.1, 29.28, 29.35, 29.46, 29.51, 31.7, 52.8, 63.3, 68.3, 112.7, 124.1, 126.0, 128.3, 129.8, 155.9, 173.3.

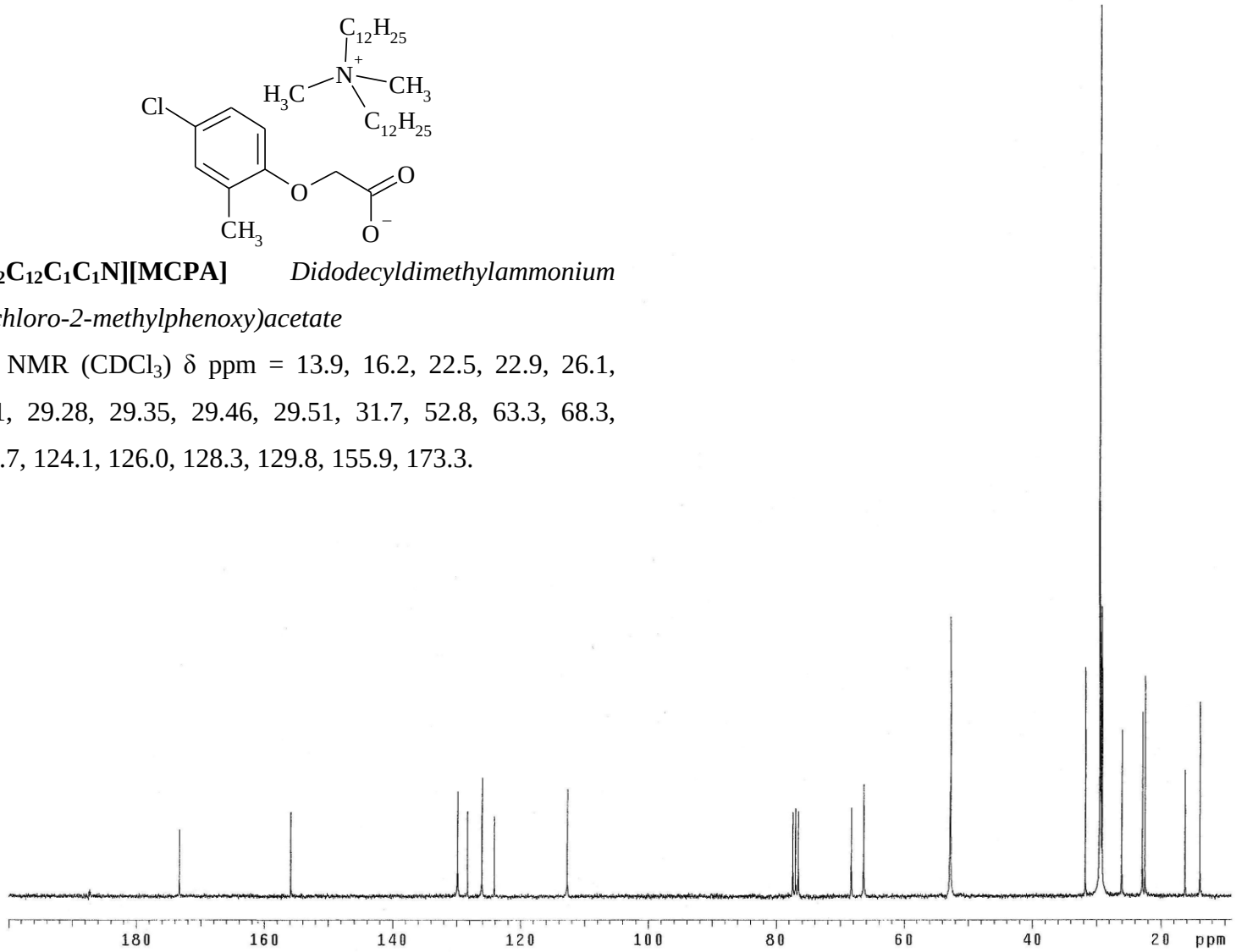

Fig. S6. ^{13}C NMR spectrum of [$C_{12}C_{12}C_1C_1N$][MCPA].

[$C_{14}C_{14}C_1C_1N$][MCPA] *Dimethylditetradecylammonium (4-chloro-2-methylphenoxy)acetate*

^{1}H NMR ($CDCl_3$) δ ppm = 0.88 (t, *J* = 6.7 Hz, 6H), 1.26 (m, 44H), 1.58 (q, *J* = 6.8 Hz, 4H), 2.23 (s, 3H), 3.07 (s, 6H), 3.14 (t, *J* = 7.8 Hz, 4H), 3.55 (H_2O), 4.40 (s, 2H), 6.71 (d, *J* = 8.5 Hz, 1H), 7.01 (dd, $J^{1,2}$= 2.6 Hz, $J^{1,3}$= 8.5 Hz, 1H), 7.04 (d, *J* = 2.6 Hz, 1H).

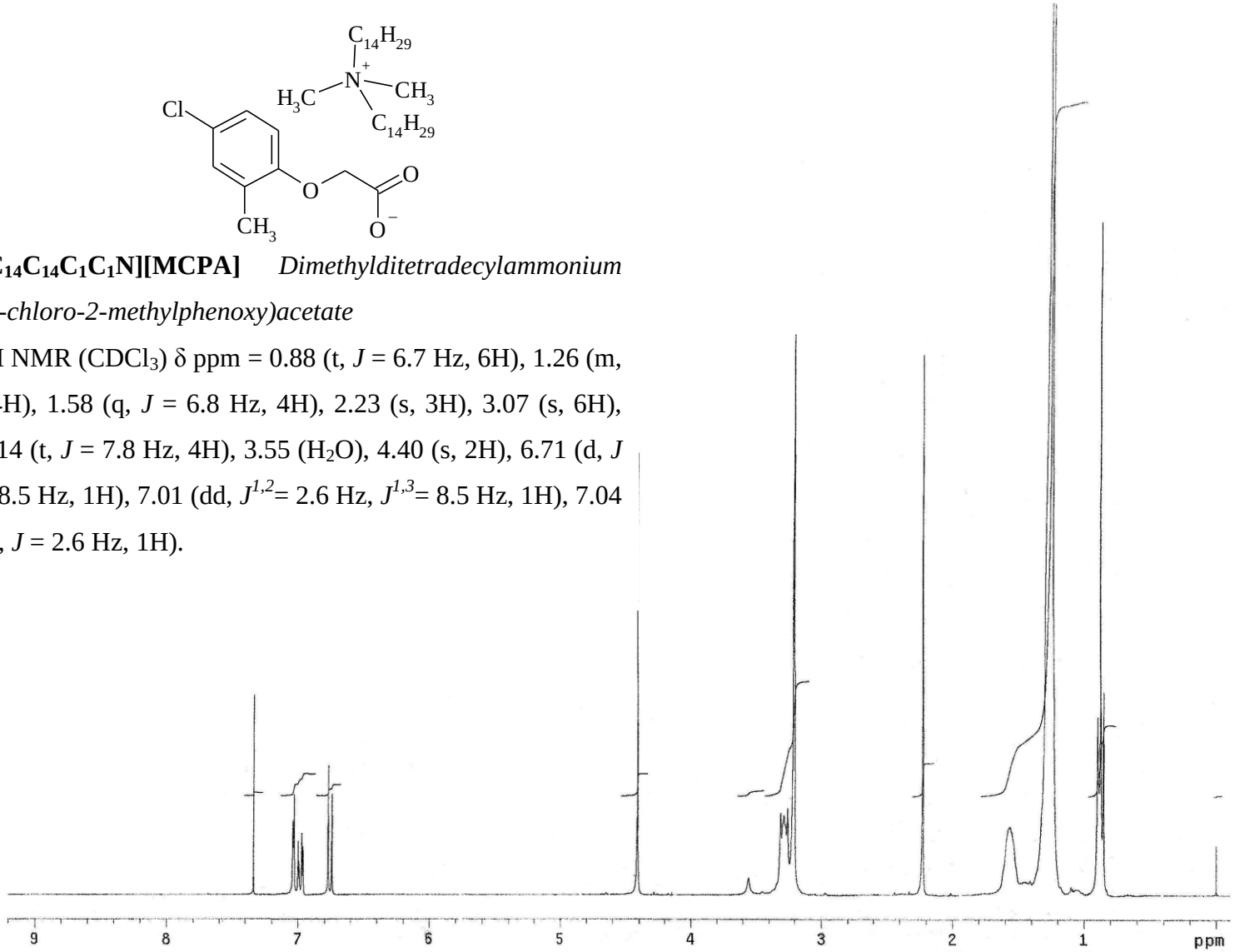

Fig. S7. ^{1}H NMR spectrum of [$C_{14}C_{14}C_1C_1N$][MCPA].

[$C_{14}C_{14}C_1C_1N$][MCPA] *Dimethylditetradecylammonium (4-chloro-2-methylphenoxy)acetate*

^{13}C NMR ($CDCl_3$) δ ppm = 14.0, 16.3, 22.46, 22.54, 26.1, 29.0, 29.22, 29.25, 29.4, 29.5, 29.6, 31.8, 51.1, 63.4, 68.1, 112.7, 124.3, 126.0, 128.5, 129.9, 155.8, 174.2.

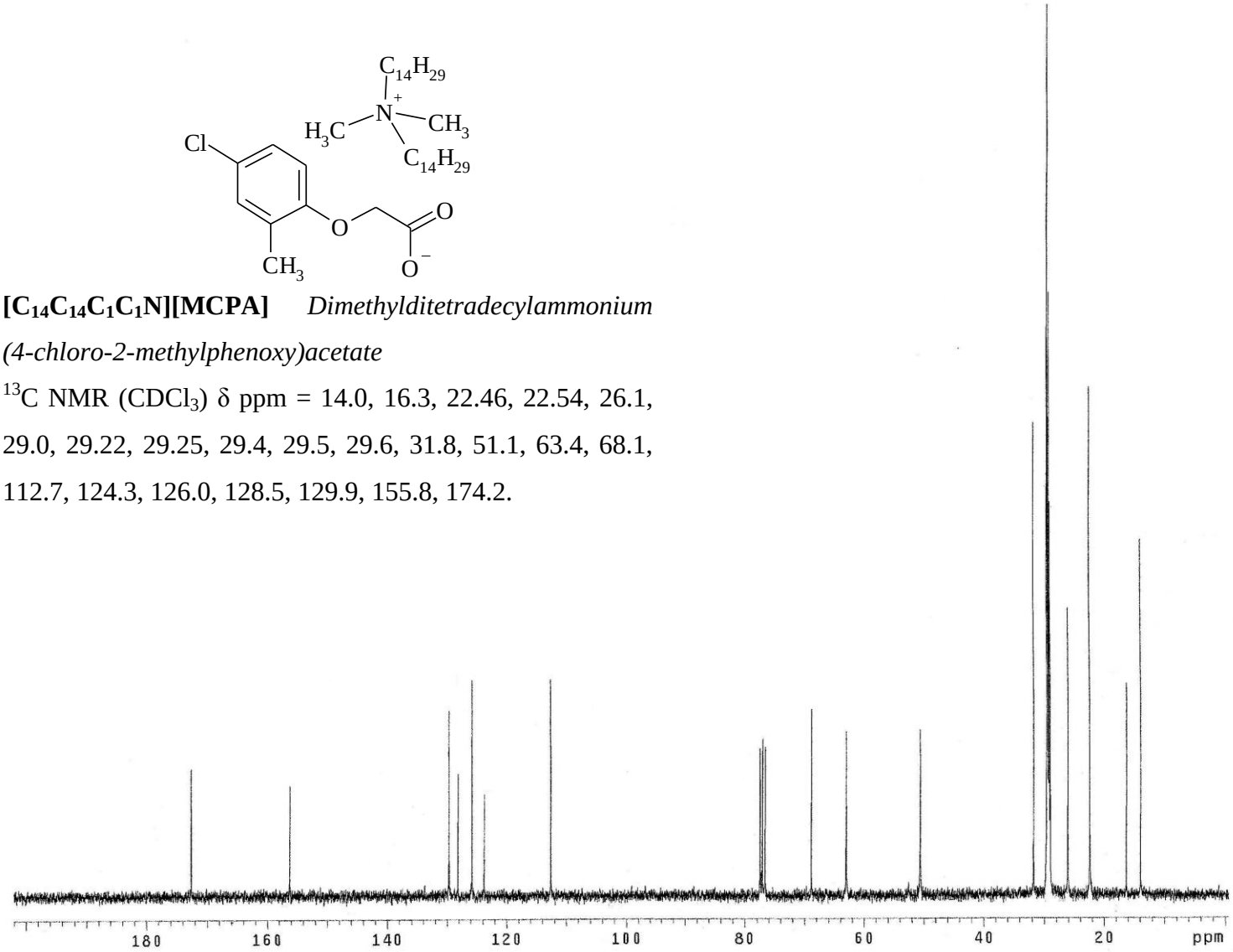

Fig. S8. ^{13}C NMR spectrum of [$C_{14}C_{14}C_1C_1N$][MCPA].

[$C_{16}C_{16}C_1C_1N$][MCPA] *Dihexyldimethylammonium (4-chloro-2-methylphenoxy)acetate*

^{1}H NMR ($CDCl_3$) δ ppm = 0.88 (t, *J* = 6.7 Hz, 6H), 1.26 (m, 52H), 1.59 (q, *J* = 6.9 Hz, 4H), 2.24 (s, 3H), 3.23 (s, 6H), 3.30 (t, *J* = 8.5 Hz, 4H), 4.41 (s, 2H), 4.62 (H_2O), 6.76 (d, *J* = 8.8 Hz, 1H), 6.99 (dd, $J^{1,2}$= 2.6 Hz, $J^{1,3}$= 8.8 Hz, 1H), 7.04 (d, *J* = 2.6 Hz, 1H).

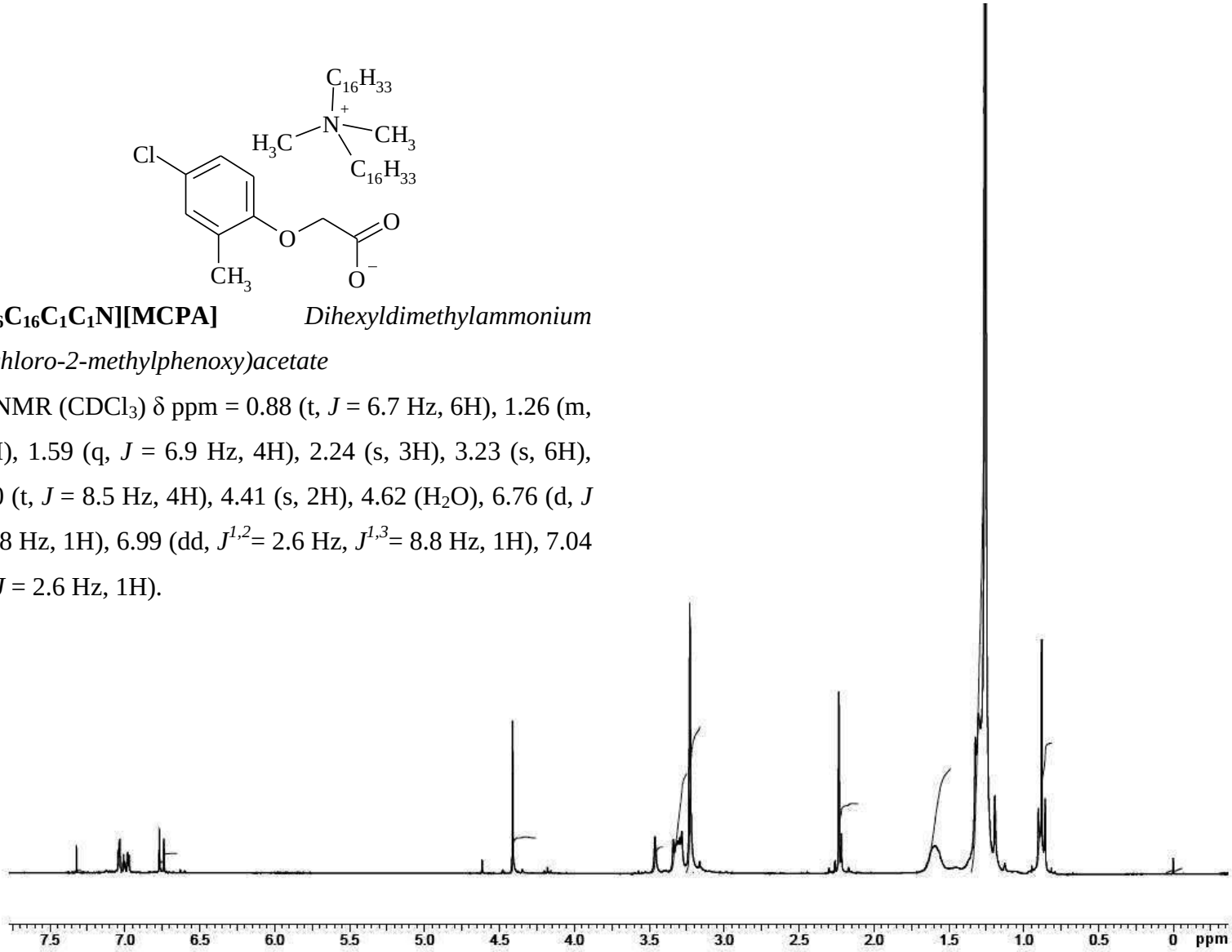

Fig. S9. ^{1}H NMR spectrum of [$C_{16}C_{16}C_1C_1N$][MCPA].

[$C_{16}C_{16}C_1C_1N$][MCPA] *Dihexyldimethylammonium (4-chloro-2-methylphenoxy)acetate*

^{13}C NMR ($CDCl_3$) δ ppm = 14.0, 16.3, 22.5, 26.1, 29.1, 29.21, 29.22, 29.34, 29.45, 29.51, 29.55, 31.8, 50.8, 63.3, 68.8, 112.7, 123.8, 125.9, 128.3, 129.8, 156.3, 172.8.

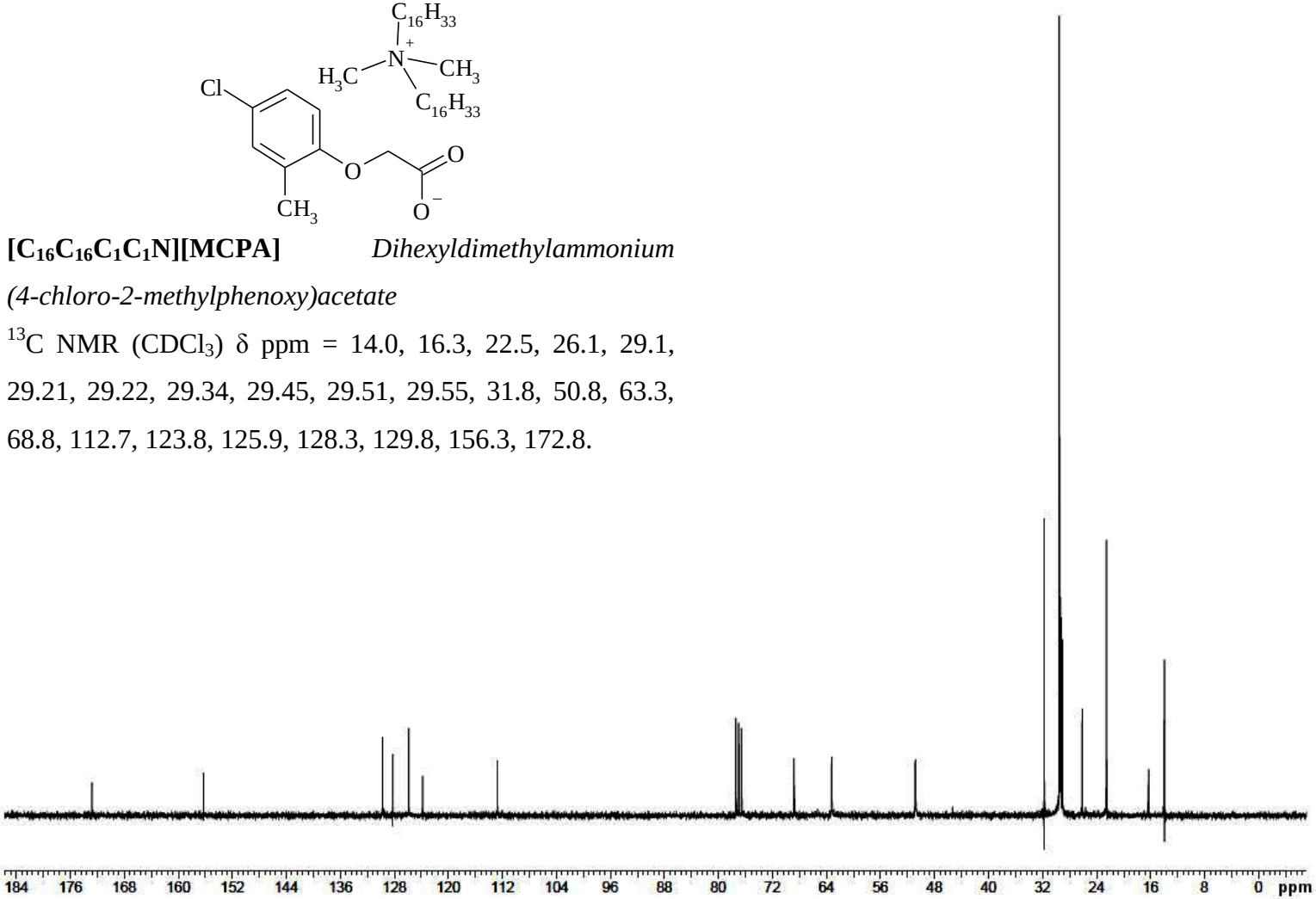

Fig. S10. ^{13}C NMR spectrum of [$C_{16}C_{16}C_1C_1N$][MCPA].

[$C_{18}C_{18}C_1C_1N$][MCPA] *Dimethydioctadecylammonium (4-chloro-2-methylphenoxy)acetate*

^{1}H NMR ($CDCl_3$) δ ppm = 0.88 (t, *J* = 6.8 Hz, 6H), 1.26 (m, 60H), 1.63 (q, *J* = 6.9 Hz, 4H), 2.21 (s, 3H), 3.28 (s, 6H), 3.37 (t, *J* = 8.3 Hz, 4H), 4.41 (s, 2H), 4.62 (H_2O), 6.76 (d, *J* = 8.8 Hz, 1H), 7.03 (dd, $J^{1,2}$= 2.6 Hz, $J^{1,3}$= 8.8 Hz, 1H), 7.10 (d, *J* = 2.6 Hz, 1H).

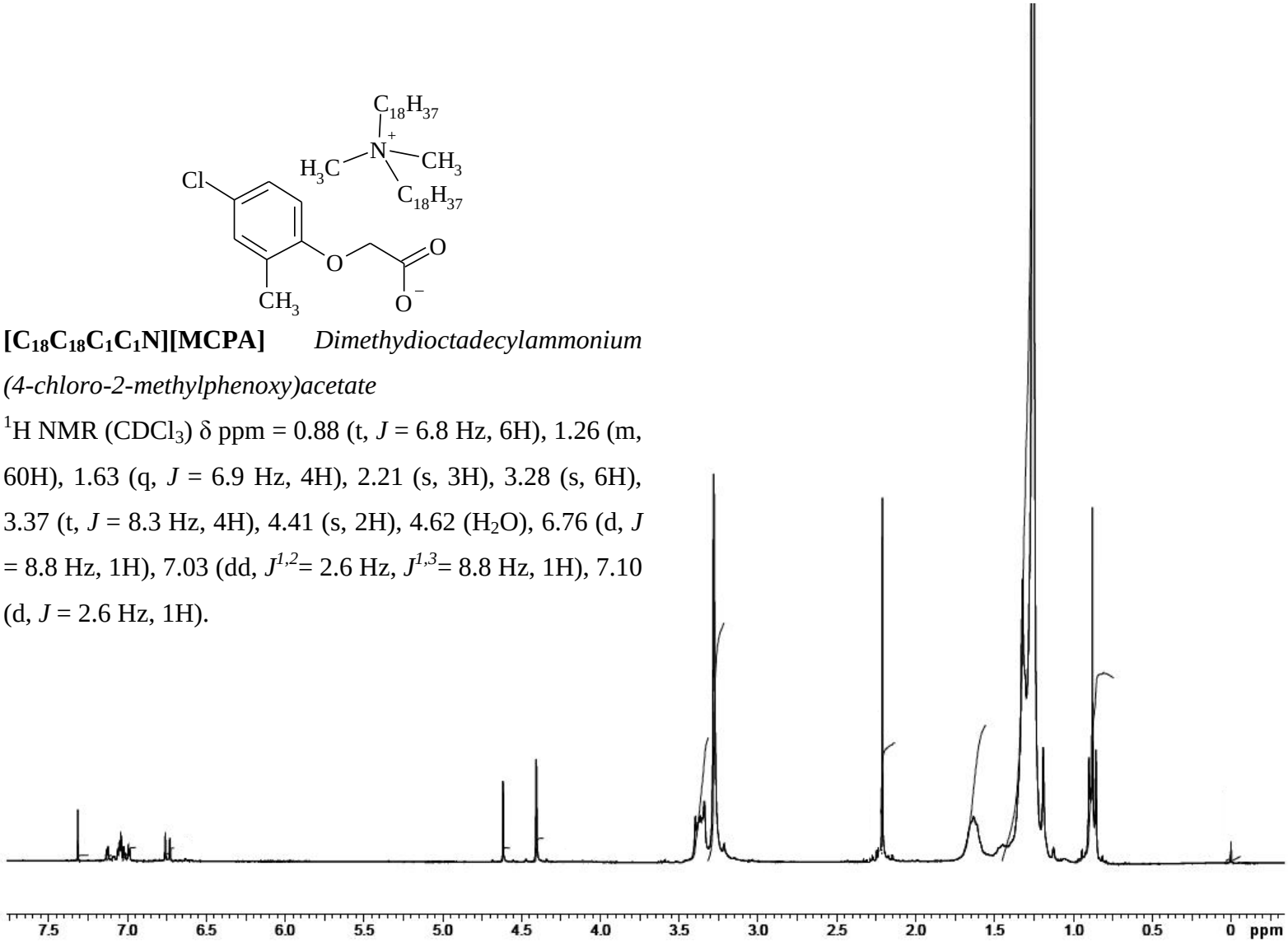

Fig. S11. ^{1}H NMR spectrum of [$C_{18}C_{18}C_1C_1N$][MCPA].

[$C_{18}C_{18}C_1C_1N$][MCPA] *Dimethydioctadecylammonium (4-chloro-2-methylphenoxy)acetate*

^{13}C NMR ($CDCl_3$) δ ppm = 14.0, 16.4, 22.6, 26.1, 29.1, 29.2, 29.3, 29.49, 29.53, 29.6, 31.8, 51.1, 63.4, 68.7, 112.7, 124.0, 126.0, 128.3, 129.8, 156.2, 173.1.

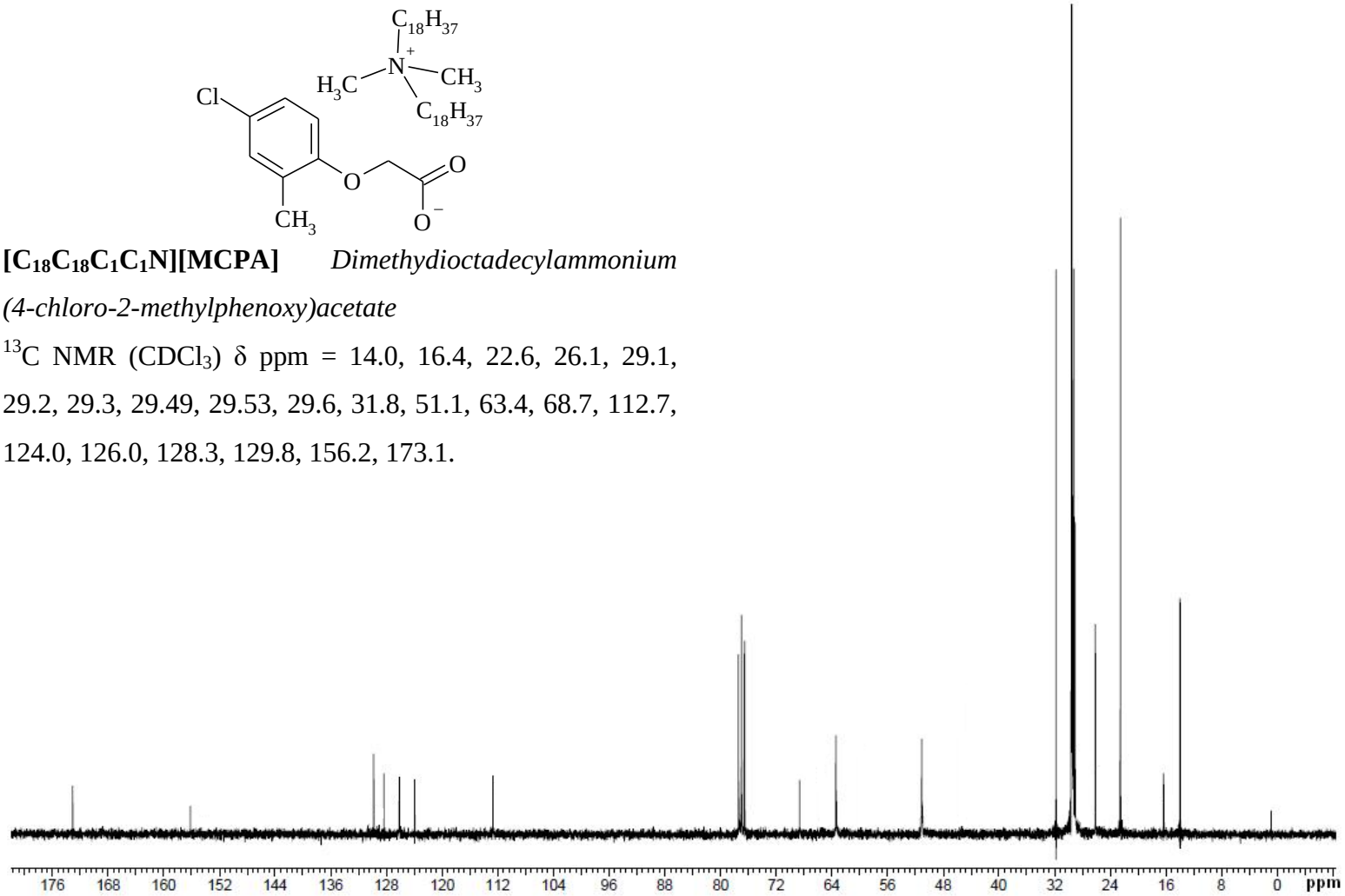

Fig. S12. ^{13}C NMR spectrum of [$C_{18}C_{18}C_1C_1N$][MCPA].

2. Electrochemical tests

2.1. Cyclic voltammetry of dialkyldimethylammonium ionic liquids with MCPA anion

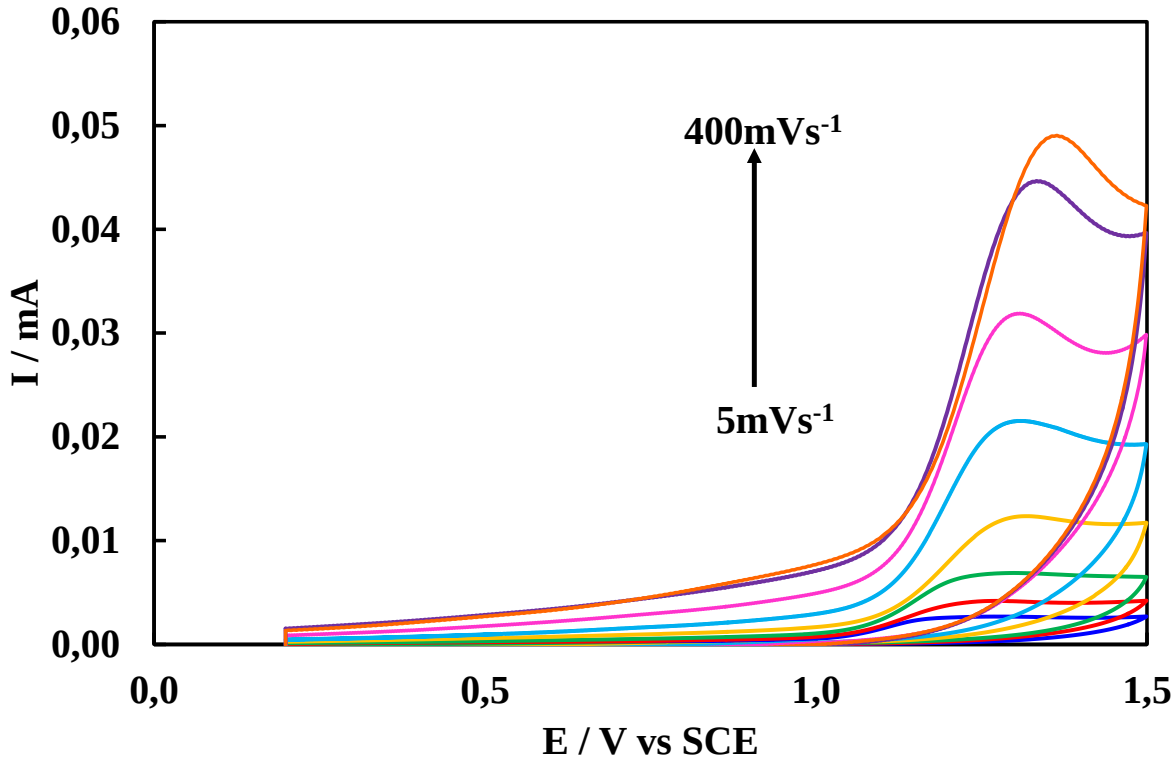

Fig. S13. Cyclic voltammetry responses of 1 mM $[C_{10}C_{10}C_1C_1N]$[MCPA] at scan rates 5 to 400mVs^{-1}.

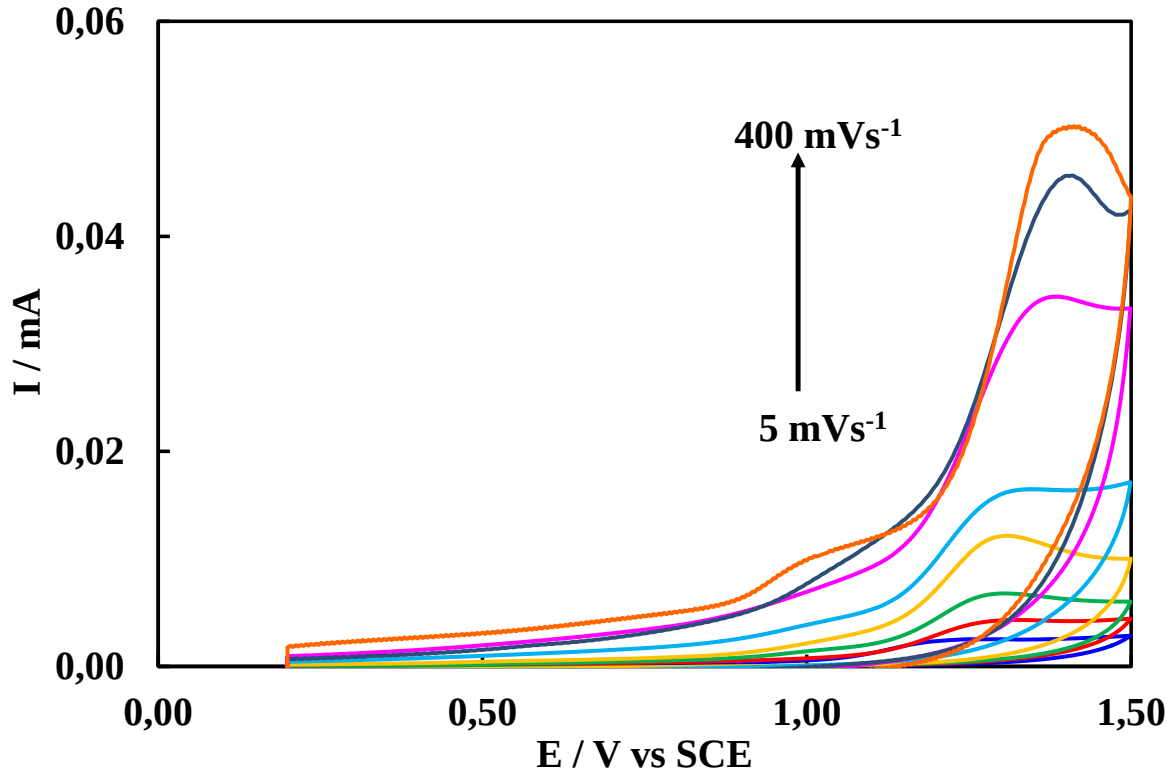

Fig. S14. Cyclic voltammetry responses of 1 mM $[C_{12}C_{12}C_1C_1N]$[MCPA] at scan rates 5 to 400mVs^{-1}.

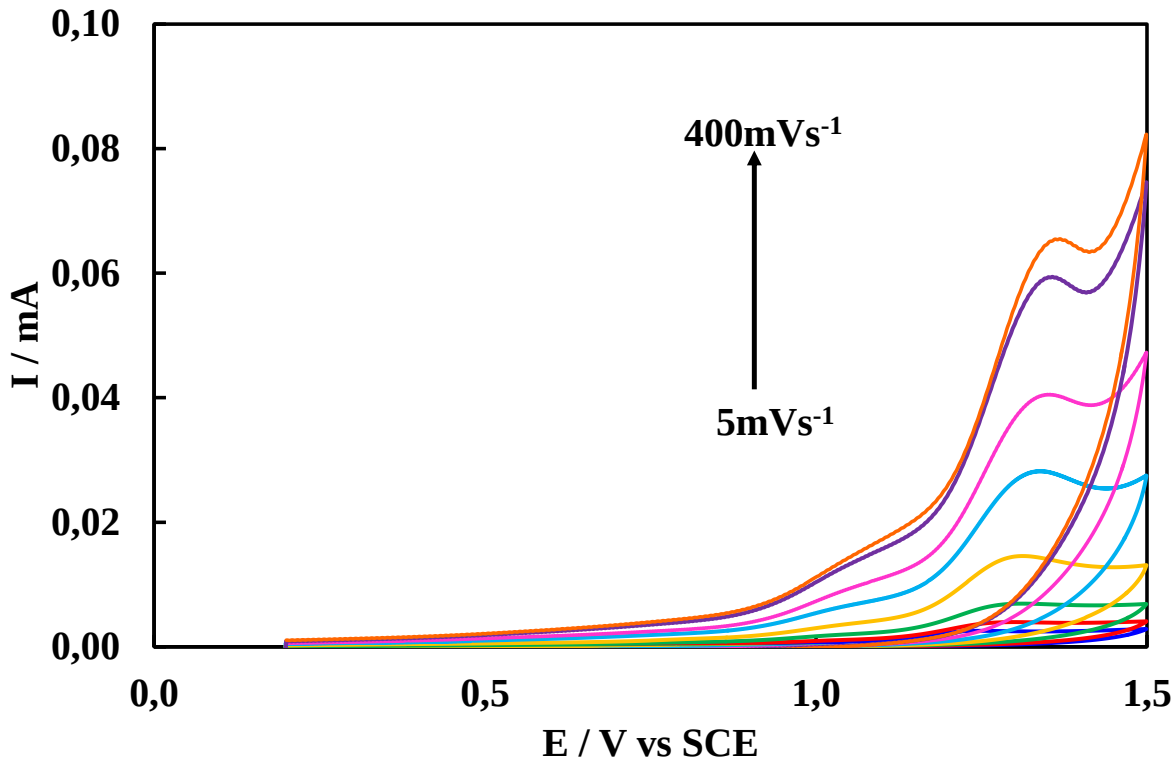

Fig. S15. Cyclic voltammetry responses of 1 mM [$C_{14}C_{14}C_1C_1N$][MCPA] at scan rates 5 to 400mVs^{-1}.

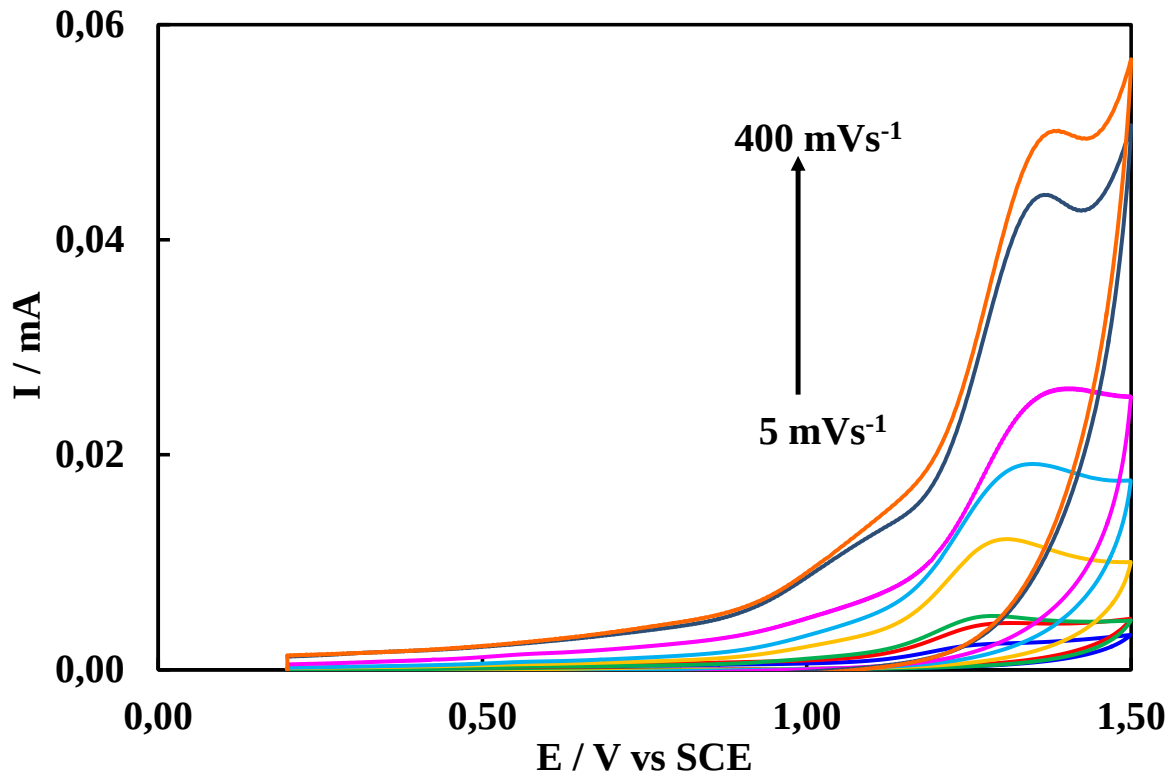

Fig. S16. Cyclic voltammetry responses of 1 mM [$C_{16}C_{16}C_1C_1N$][MCPA] at scan rates 5 to 400mVs^{-1}.

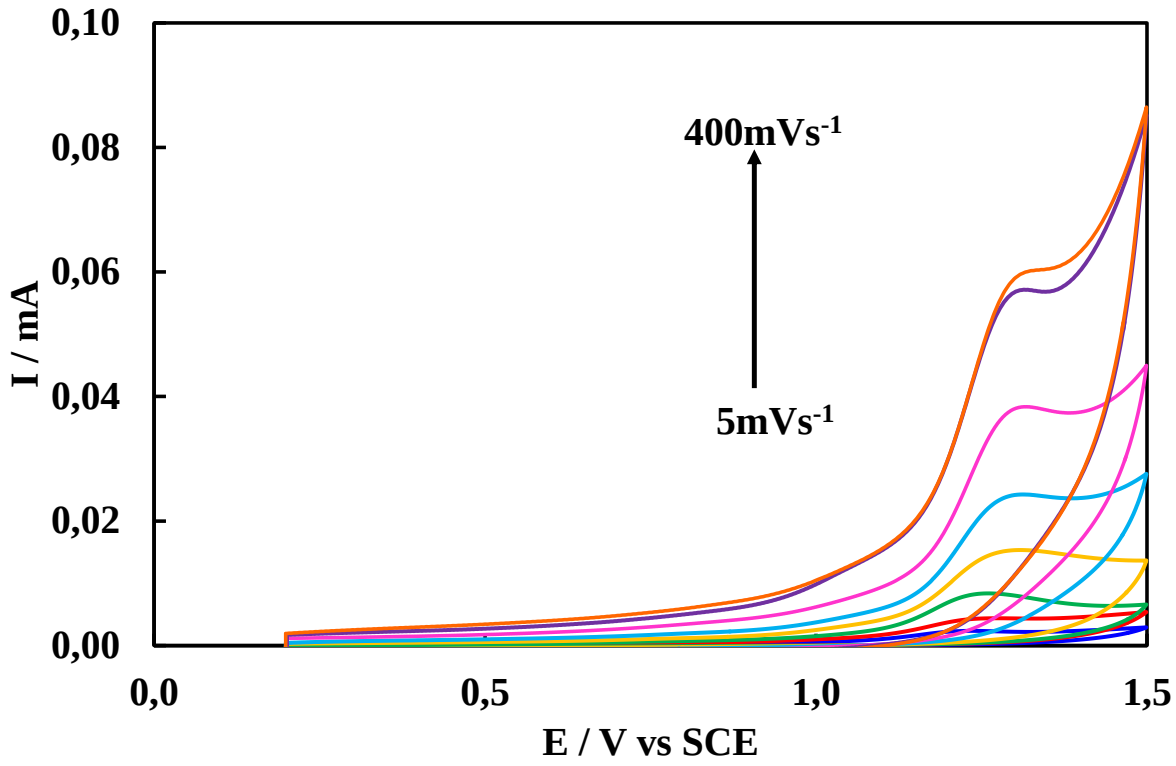

Fig. S17. Cyclic voltammetry responses of 1 mM $[C_{18}C_{18}C_1C_1N]$[MCPA] at scan rates 5 to 400mVs^{-1}.

2.2. The dependence between the potential and scan rate obtained for the dialkyldimethylammonium ionic liquids with MCPA anion

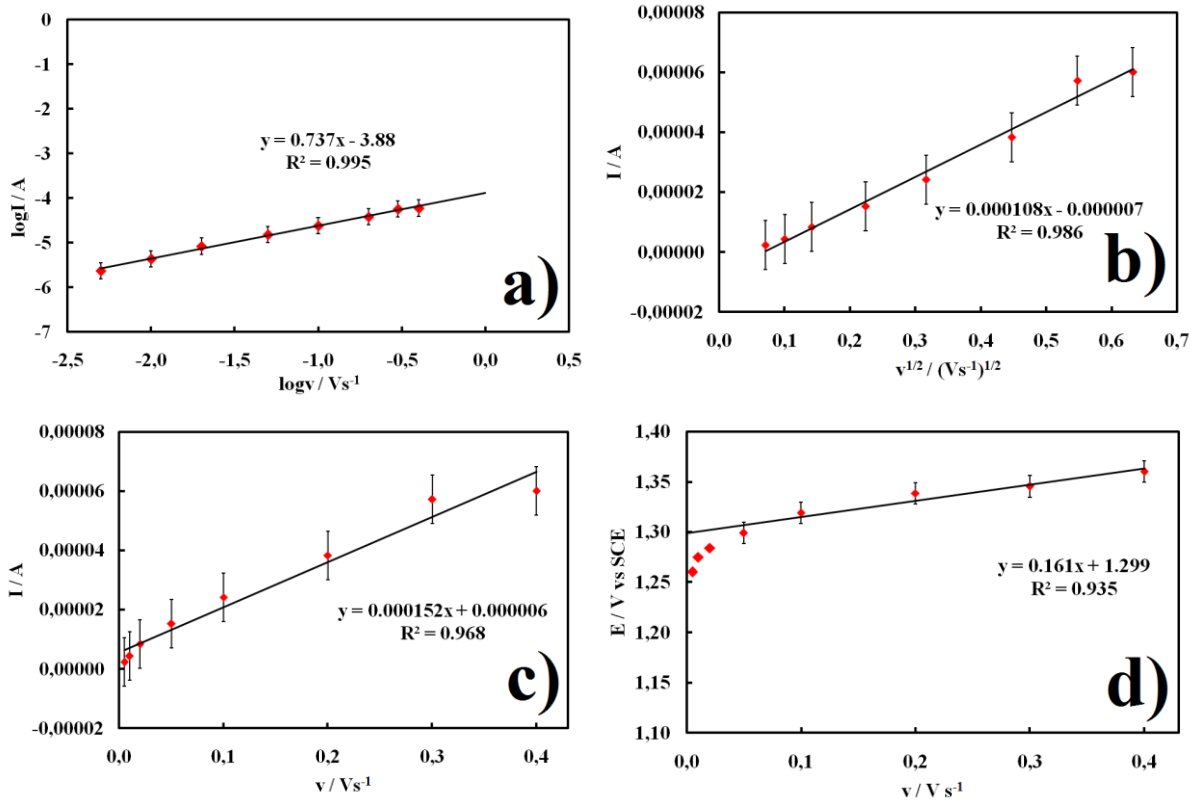

Fig. S18. a) The dependence between the potential and scan rate obtained for [$C_{10}C_{10}C_1C_1N$][MCPA] which present a) peak current logarithm**;** b) maximal peak current; c) maximal peak current and d) oxidation potential versus scan rate.

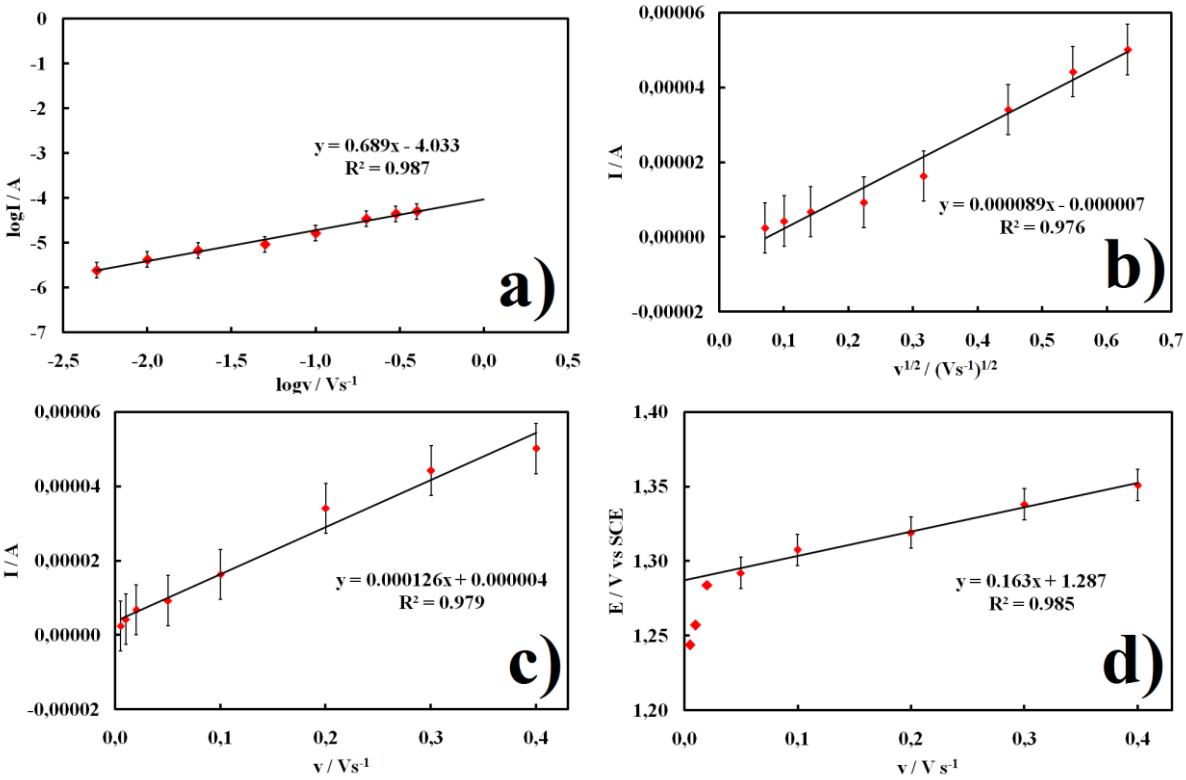

Fig. S19. a) The dependence between the potential and scan rate obtained for $[C_{12}C_{12}C_1C_1N]$[MCPA] which present a) peak current logarithm**;** b) maximal peak current; c) maximal peak current and d) oxidation potential versus scan rate.

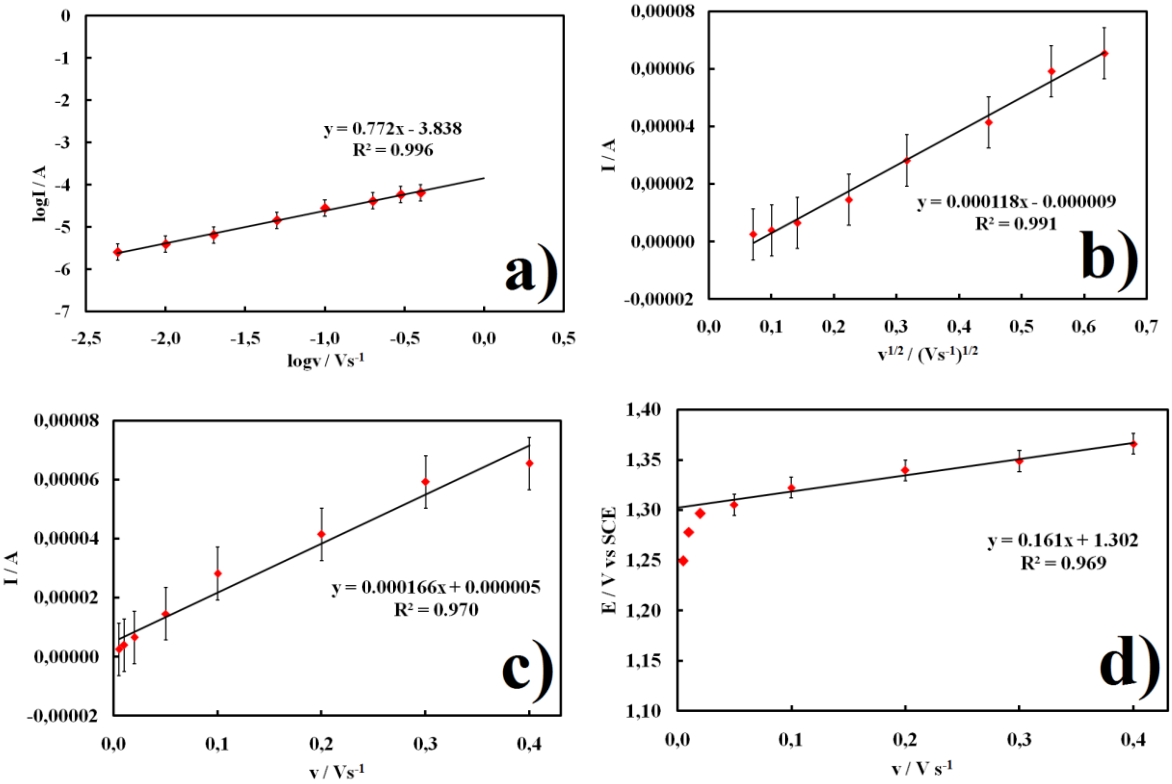

Fig. S20. a) The dependence between the potential and scan rate obtained for $[C_{14}C_{14}C_1C_1N]$[MCPA] which present a) peak current logarithm**;** b) maximal peak current; c) maximal peak current and d) oxidation potential versus scan rate.

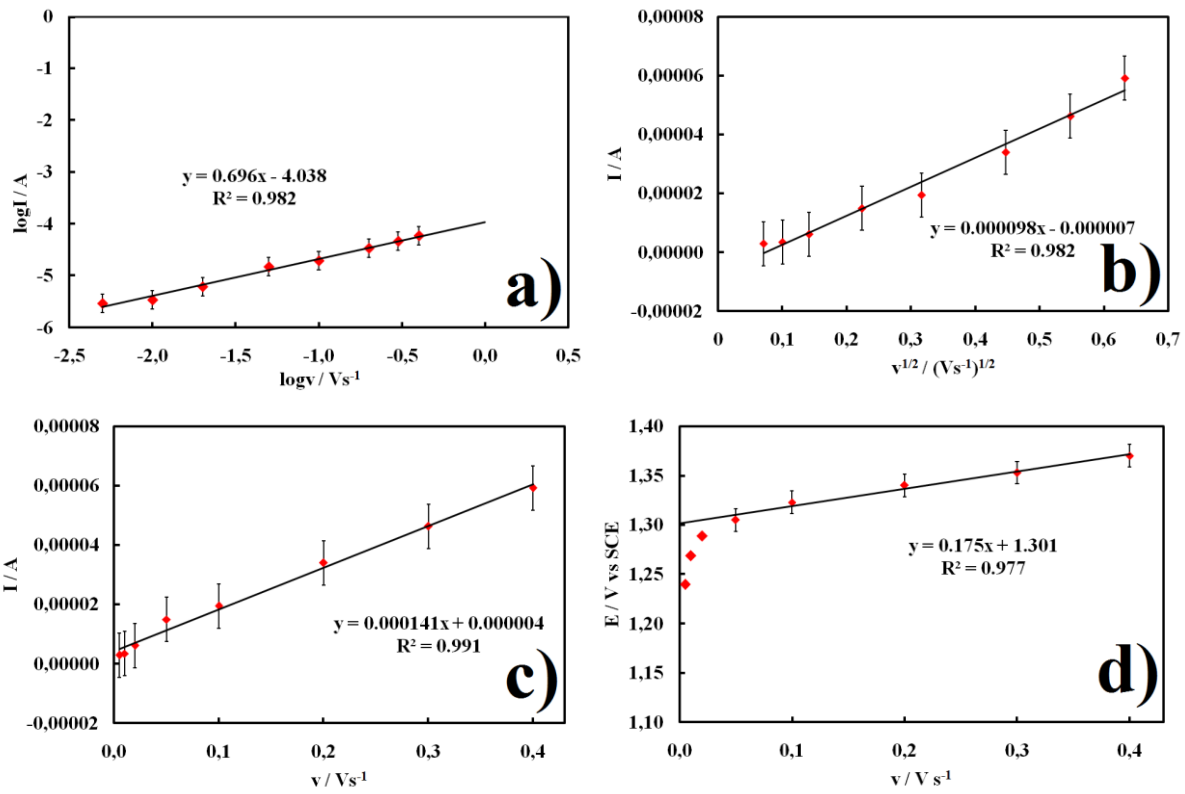

Fig. S21. a) The dependence between the potential and scan rate obtained for $[C_{16}C_{16}C_1C_1N]$[MCPA] which present a) peak current logarithm**;** b) maximal peak current; c) maximal peak current and d) oxidation potential versus scan rate.

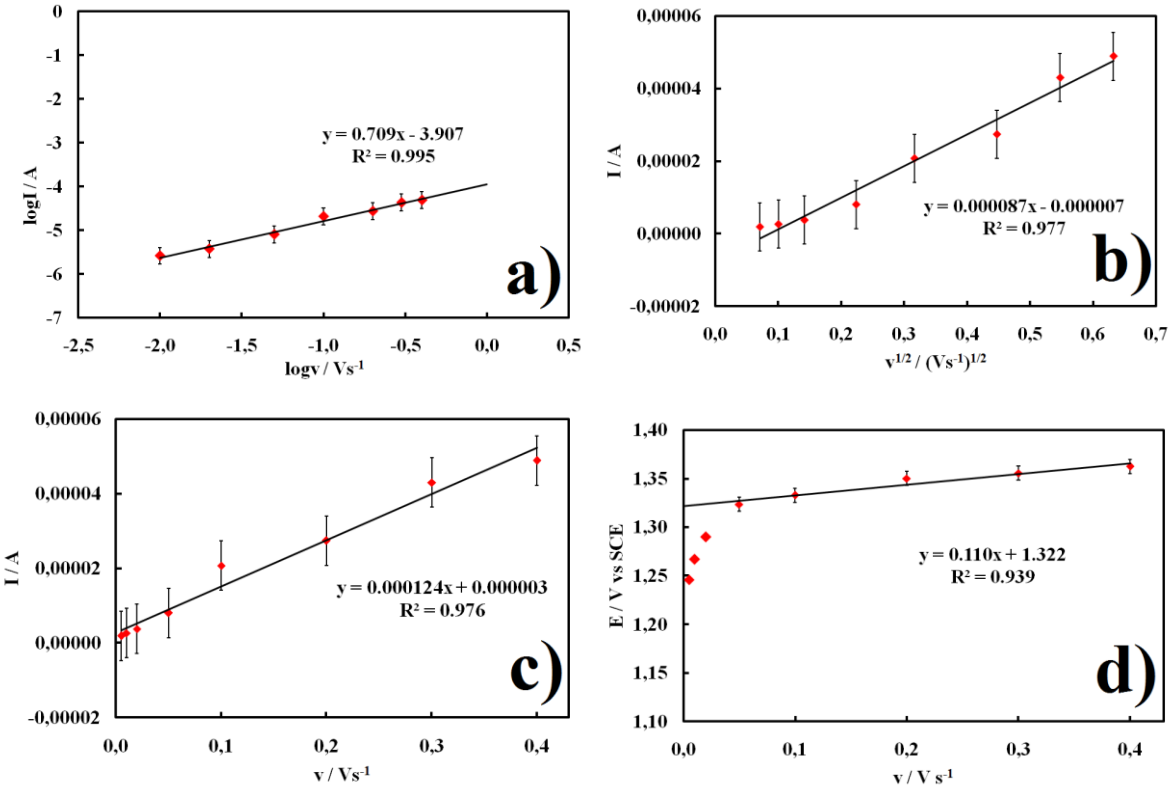

Fig. S22. a) The dependence between the potential and scan rate obtained for $[C_{18}C_{18}C_1C_1N]$[MCPA] which present a) peak current logarithm**;** b) maximal peak current; c) maximal peak current and d) oxidation potential versus scan rate.

2.3. Characterization of the oxidation process

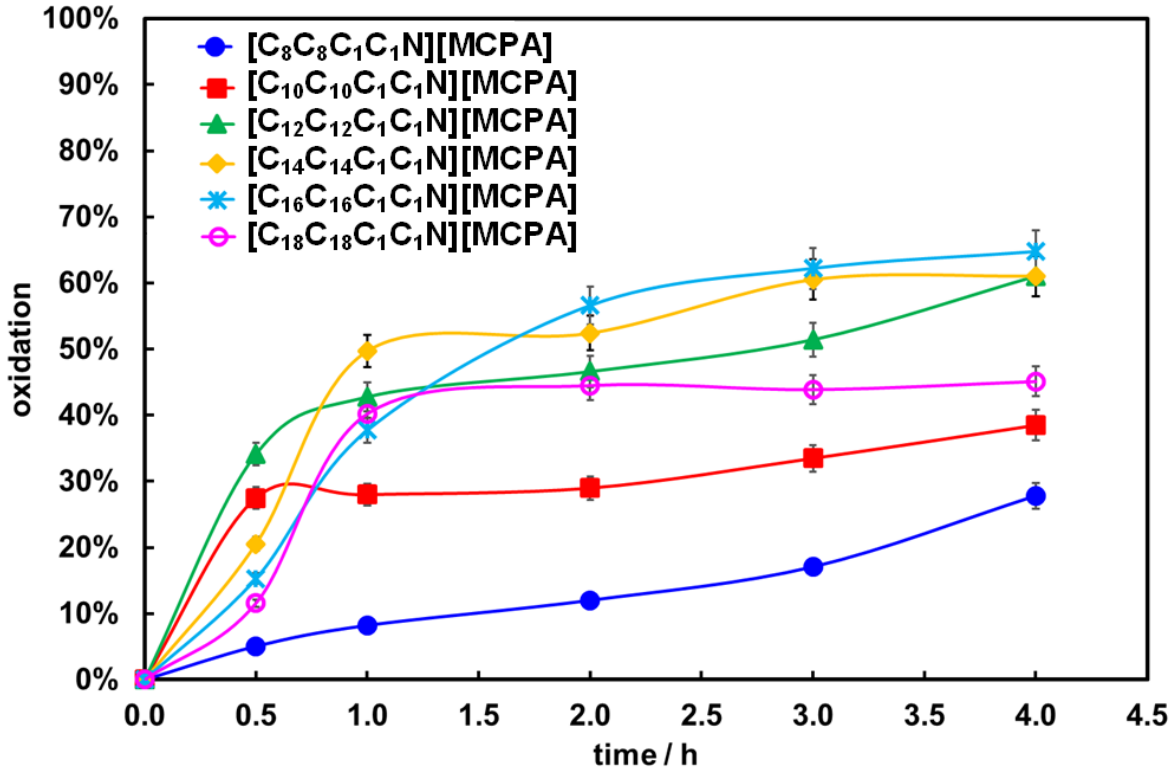

Fig. S23. The oxidation state of studied HILs during the electrochemical oxidation process.

2.4. BOD_5 and COD values of non-treated and electrochemically treated samples

Table S1. Values of BOD_5 for electrochemically treated and non-treated samples.

	BOD_5/COD
Non-treated [$C_8C_8C_1C_1N$][MCPA]	0.192
Electrochemically treated [$C_8C_8C_1C_1N$][MCPA]	0.259
Non-treated [$C_{10}C_{10}C_1C_1N$][MCPA]	0.149
Electrochemically treated [$C_{10}C_{10}C_1C_1N$][MCPA]	0.255
Non-treated [$C_{12}C_{12}C_1C_1N$][MCPA]	0.144
Electrochemically treated [$C_{12}C_{12}C_1C_1N$][MCPA]	0.335
Non-treated [$C_{14}C_{14}C_1C_1N$][MCPA]	0.163
Electrochemically treated [$C_{14}C_{14}C_1C_1N$][MCPA]	0.454
Non-treated [$C_{16}C_{16}C_1C_1N$][MCPA]	0.165
Electrochemically treated [$C_{16}C_{16}C_1C_1N$][MCPA]	0.459
Non-treated [$C_{18}C_{18}C_1C_1N$][MCPA]	0.179
Electrochemically treated [$C_{18}C_{18}C_1C_1N$][MCPA]	0.341

References

Cross, J.T., 1965. The identification and determination of cationic surface-active agents with sodium tetraphenylboron, *Analyst.* 90, 315–324.

Wang, D.-H., Weng, H.-S., 1995. Solvent and salt effects on the formation of third liquid phase and the reaction mechanisms in the phase transfer catalysis system-reaction between n-butyl bromide and sodium phenolate, Chem. Eng. Sci., 50, 3477–3486.